이학박사 학위논문

Hyperbolic volume potential functions and knotted graph complements

(쌍곡 부피 잠재함수와 매듭진 그래프 여공간)

2013년 8월

서울대학교 대학원

수리과학부

김 선 화

Hyperbolic volume potential functions and knotted graph complements

A dissertation
submitted in partial fulfillment
of the requirements for the degree of
Doctor of Philosophy
to the faculty of the Graduate School of
Seoul National University

by

Seonhwa Kim

Dissertation Director : Professor Hyuk Kim

Department of Mathematical Science
Seoul National University

August 2013

Abstract

Hyperbolic volume potential functions and knotted graph complements

Seonhwa Kim

Department of Mathematical Sciences
The Graduate School
Seoul National University

Optimistic limit method of quantum invariants has been developed from an attempt to solve the Kashaev volume conjecture. Although it may seem to be hard to formulate in a rigorous way, this method produces explicit correct volume formulas of hyperbolic links, which are given by the critical values of the potential functions written directly from the link diagrams. In this dissertation, we study a sufficient condition to produce hyperbolic volumes of $PSL(2,\mathbb{C})$-representations as critical values of a certain type of functions and also define a volume potential function to obtain hyperbolic volume of the knotted graph complement considering generalized octahedral decomposition.

Key words: Volume Conjecture, Quantum topology, Hyperbolic geometry, Low dimensional topology, Graph
Student Number: 2004-23257

Contents

List of Figures

Introduction

Volume conjecture is a statement about a certain relationship between asymptotic behaviors of quantum invariant like colored Jones polynomial and classical geometric invariant like hyperbolic volume, Chern-simons invariant, A-polynomial and so on. Thesedays there are various versions of volume conjectre. The original one is Kashaev volume conjecture in [14] which states the following.

$$\mathrm{vol}(L) = 2\pi \lim_{N\to\infty} \frac{\log|\langle L\rangle_N|}{N}$$

where L is a hyperbolic link and $\langle L\rangle_N$ is the Kashaev invariant of L which is the same as evaluation of the colored Jones polynomial at $e^{\frac{2\pi\sqrt{-1}}{N}}$.

Among the results for knotted graph revealing similar relationship are several volume formulas in [20], [21], [22] by J. Murakami which produce the volume of hyperbolic or spherical tetrahedron by its dihedral angles or edge lengths. These formulas come from asymptotics of quantum $6j$-symbols. Moreover, Van der Veen's result [27] shows that volume conjecture is true for tetrahedron descendant graphs and augmented links, in which case their volumes coincide with multiples of the regular hyperbolic ideal octahedron's volume. More generally, quantum spin networks are also expected to give hyperbolic volumes of general knotted trivalent graph complements as their certain asymptotics. Recently, an evidence of deeper relationships has been revealed; asympototics of quantum representations are related to not only hyperbolic volumes and Chern-Simons invariants but also Reidemister torsions, $PSL(2,\mathbb{C})$-character variety of the knot group and so on ([7], [8], [10]).

In the previous work [2] with Jinseok Cho and Hyuk Kim, we suggest a volume formula for a hyperbolic link L using an optimistic limit method for Kashaev invariant whose original form comes from Y. Yokota's work [29]. Although the origin of this formula comes from a quantum invariant [30], the statement is purely combinatorial and involves none of quantum group representation or Chern-Simons theory and the proof only needs hyperbolic geometry and extended Bloch group theory of W. Neumann [23] and C. Zickert [31].

Main result of this dissertation is a generalization of the earlier work to knotted graphs. A knotted graph means a smooth embedding of a graph into S^3 and is also called as spatial graphs or spatial networks in different fields such as biology and computer science.

Definition. A knotted graph G is called hyperbolic if $S^3 \setminus \{G \bigcup N(V(G))\}$ admits a *pared* hyperbolic structure which has totally geodesic boundaries of punctured spheres and annular cusps, corresponding to vertices $V(G)$ and edges $E(G)$, respectively ([12]). Volume of G means volume of the pared hyperbolic manifold of its complementary space, denoted by $\mathrm{vol}(G)$.

Meanwhile, quantum spin network evaluation can be considered as a generalization of colored Jones polynomial to trivalent knotted graphs (called KTG). It is already known that in several cases the hyperbolic volumes of the complements appear as their asymptotics ([27]).

One of the obstacles to investigating these relationships is an absence of volume formula for KTG graph complements. In order to resolve this problem, we constuct a volume potential function for knotted graphs as a generalization of optimistic limit of Kashaev invariants.

At first, define a multi-valued complex function

$$V_G : (\mathbb{C} \setminus 0)^n \longrightarrow \mathbb{C},$$

where each complex variable is assigned to a segment of a diagram of G and n is the number of segments. Here, the term *segment* has the same meaning as *side* in [2] or *edge* in [30]. we reserve the term *edge* for the triangulation and the abstract graph. V_G is a summation of dilogarithm functions at each corner as a rule depicted in the figure 1, and has lots of singularities. Let $\widetilde{V_G}$ be a complex single-valued function on a certain Riemann domain by analytic continuation of V_G. Then we can obtain the following theorem.

Theorem. Let G be a hyperbolic knotted graph. V_G is a complex multi-valued function defined by the rule in the following figure 1. If there is a critical point except for singularities of V_G, then

$$\mathrm{Im}\widetilde{V_G}(\widetilde{\zeta}) = \mathrm{Im}\widehat{V_G}(\zeta) = \mathrm{vol}(G),$$

where $\widehat{V}$ is a compensated evaluation (see definition 1.3) and $\widetilde{\zeta}$ is a critical point of $\widetilde{V_G}$ at which the value of $\mathrm{Im}\widetilde{V_G}$ is maximal.

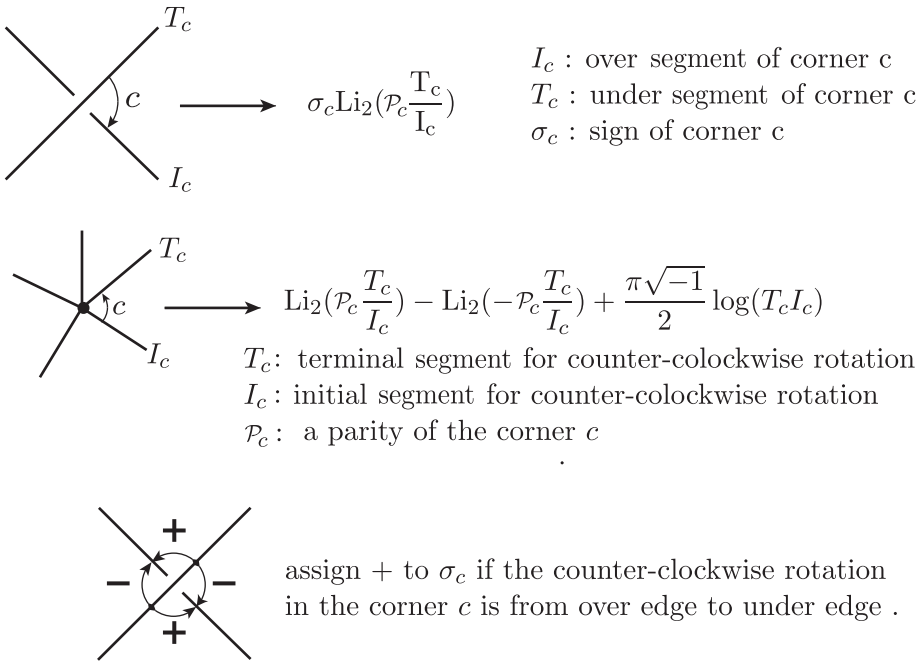

Figure 1: Defining rule for volume potential V_G

Where a corner parity $\mathcal{P}_c$ is defined by $\mathcal{P}_G(c)$ of the following definition. we will investigate the more detailed concept of corner parity system in section 3.

Definition. A corner parity system $\mathcal{P}_G$ for a plane diagram G is defined by a function from the set of all corners $\mathcal{C}$ to $\{+1, -1\}$ satisfying the following two properties.

$$1) \quad \prod_{c \text{ meets } v} \mathcal{P}_G(c) = (-1)^{\deg v} \quad \text{for all vertex } v \in G$$

$$2) \quad \prod_{c \text{ meets } f} \mathcal{P}_G(c) = 1 \quad \text{for all faces } f \in G$$

In particular, a corner parity system exists always for any knotted graph diagram by theorem 2.13 and all corner parity systems produce equivalent potential functions by theorem 2.15.

Note that the volume formula holds for the more general knotted graphs than just trivalent graphs. I think this fact is an evidence that quantum spin network evaluation might be generalized for the more general knotted graphs.

Chapter 0

Preliminaries

0.1 Dilogarithm and hyperbolic volume

Definition 0.1. The *dilogarithm function* is a complex function defined by an analytic continuation of a power series $\sum_{n=1}^{\infty} \frac{z^n}{n^2}$ ($|z| \leq 1$) and written in the following contour integral

$$\mathrm{Li}_2(z) := -\int_0^z \frac{\log(1-t)}{t} dt \tag{0.1}$$

Note the the dilogarithm is a multi-valued function and usually depends on the choice of a contour C from 0 to z. $\mathrm{Li}_2{}^*(z)$ and $\log^* z$ denote the principal branch of $\mathrm{Li}_2(z)$ and $\log z$ repectively, with branch choice of $-\pi < \arg(z) \leq \pi$. The other brances of $\mathrm{Li}_2(z)$ is written in the term of the principal branch by

$$\mathrm{Li}_2(z) = \mathrm{Li}_2{}^*(z) + 2n\pi\sqrt{-1}\log^*(z) + 4m\pi^2, \tag{0.2}$$

in which $n, m \in \mathbb{Z}$. we note that n is the winding number around $1 \in \mathbb{C}$ and m is determined by more complicated way [17].

Let $f(z)$ be a multi-valued function on an open set in $\mathbb{C}^n$. We can define $\widetilde{f}(\widetilde{z})$ as a single valued function on a certain Riemann domian X by analytic continuation beyond $\mathbb{C}^n$. The Riemann domain X can be considered as an complex manifold where branch choices of f produce a system of holomorphic coordinate charts on X.

Since $\mathrm{Li}_2(z)$ is a multi-valued function we can analytically continue to beyond complex plane $\mathbb{C}$ and get a single valued function $\widetilde{\mathrm{Li}_2}(\tilde{z})$ on a certain Riemann surface X where $\widetilde{z}$ denotes an point of X, which is determined by a homotopy class of a contour $C : [0,1] \longrightarrow \mathbb{C} \setminus \{0,1\}$ with $C(1) = z$.

$$\widetilde{\mathrm{Li}_2}(\widetilde{z}) := -\int_C \frac{\log(1-t)}{t} dt \tag{0.3}$$

Definition 0.2 (shape parameter)**.** Hyperbolic ideal tetrahedron can be parametrized by a complex number $z \in \mathbb{C} \setminus \{0, 1\}$ with a choice of vertex ordering (z_1, z_2, z_3, z_4). The vertices of a ideal tetrahedron indicate complex numbers in $\mathbb{C} \cup \{\infty\}$ as points in the ideal boundary of $\mathbb{H}^3$. the cross-ratio is invariant under hyperbolic isometries.

$$[z_0, z_1, z_2, z_3] = \frac{(z_0 - z_3)(z_1 - z_2)}{(z_0 - z_2)(z_1 - z_3)} =: z \tag{0.4}$$

We call this complex number z as *shape parameter* of a tetrahedron T_z.

Definition 0.3 (*Bloch-Wigner function)***.**

$$D(z) := \mathrm{Im}\mathrm{Li}_2(z) + \log|z| \arg(1 - z) \tag{0.5}$$

It is to be noted that Bloch-Wigner function $D(z)$ is independent from the branch choice of $\mathrm{Li}_2(z)$ and give hyperbolic volume of ideal tetrahedra as the following proposition.

Proposition 0.4 (volume of ideal tetrahedron [26],[15])**.** *Let z be a shape parameter of tetrahedron T_z, then*

$$\mathrm{vol}(T_z) = D(z)$$

0.2 Gluing equation and $PSL(2, \mathbb{C})$-representations

Main references of this section is [16],[24], [25], [26]. Let M be an oriented manifold which is obtained by gluing of finite number simplices with deleted vertices.

$$M = \Delta_1 \cup \Delta_2 \cup ... \cup \Delta_m$$

Let $\mathcal{T}$ be the ideal treangulation for M possibly with trivial sphere cusp and $G_{\mathcal{T}}$ be the hyperbolicity equation for $(M, \mathcal{T})$. $\mathcal{S}$ denotes the solution set of $G_{\mathcal{T}}$.

Theorem 0.5. *Each $\zeta \in \mathcal{S}$ gives a representation $\rho_\zeta : \pi_1(M) \longrightarrow PSL(2, \mathbb{C})$, and* $\mathrm{vol}(\rho_\zeta) = \sum_{k=1}^{m} D(\Delta_k)$.

sketch of proof. By Poincare polyhedron theorem, $\pi_1(M)$ can be generated by face gluing of $\mathcal{T}$ and we can interprete every cycle in $\pi_1(M)$ as a product of edges of Δ_k. Since every edge in ideal hyperbolic tetrahedra corresponds a certain loxodromic isometry in $\mathbb{H}^3$, Edge paths of dual 1-skeleton in $\mathcal{T}$ correspond the elements of $PSL(2, \mathbb{C})$ □

Theorem 0.6 (Corollay 7.3 in [9])**.** *If one assume $\mathcal{S} \neq \emptyset$, then $\mathcal{S}$ must have discrete faithful representation of M. Therefoe a maximal evaluation of $\sum_{k=1}^{m} D(\Delta_k)$ on $\mathcal{S}$ produces the hyperbolic volume of M by Gromov-Goldman-Thurston rigidity.*

Chapter 1

Volume Potential function

1.1 Volume conjecture

Volume conjecture[14] means simply that the following equaility.

$$\mathrm{vol}(L) = 2\pi \lim_{N\to\infty} \frac{\log|\langle L\rangle_N|}{N} \tag{1.1}$$

where L is a hyperbolic link and $\langle L\rangle_N$ is Kashaev invariant of L which is equal to colored Joiones polynomial at $e^{\frac{2\pi\sqrt{-1}}{N}}$ [19].

Various generalization is possible, for example, using complex volume i.e. hyperbolic volume + $\sqrt{-1}$ Chern-Simons invariant or Gromov's simplical norm for non-hyperbolic link. Moreover it seems to be naturally appeared that twisted Reidemeister torsion and unknown topological invariants in full asympotics expansions. Many quantum invariants like, for example, quantum 6j-symbols, Turaev-Viro invariants, and quantum A-polynomial also expected that have similar relationship with a certain classical geometric invariants. But the most of those are still conjecture. There is a nice introductory article [6], [18].

1.2 Optimistic limits

To avoid struggling complicated notations and lots of indexes, we will summarize them a little bit excessively and omit many things except key ideas. At first, Kashaev invariant is defined by the following expression.

$$\langle L\rangle_N = \mathrm{Tr}\prod \text{Kashaev R-matrix} \times \text{less-important other terms}$$

Kashaev R-matrix's entries mainly consist of q-series $(q)_k = (1-q)(1-q^2)...(1-q^k)$ with $q = e^{\frac{2\pi\sqrt{-1}}{N}}$, so we can write in the following manner.

$$\langle L\rangle_N = \sum_{k_1,k_2,...,k_m} \prod (q)_{k_i - k_j} \times \text{other terms} \tag{1.2}$$

q series have following estimation.

$$(q)_k = \quad \exp(\tfrac{N}{2\pi\sqrt{-1}}(\tfrac{\pi^2}{6} - \mathrm{Li}_2(e^{\frac{2\pi\sqrt{-1}k}{N}})) + other_{n,k})) \tag{1.3}$$

$$(q)_k^* = \quad \exp(\tfrac{N}{2\pi\sqrt{-1}}(-\tfrac{\pi^2}{6} + \mathrm{Li}_2(e^{\frac{2\pi\sqrt{-1}k}{N}})) + other_{n,k})) \tag{1.4}$$

where, $|other_{n,k}| \sim \log N$ as $N \longrightarrow \infty$ when $\frac{k}{N}$ is fixed.

$$\langle L\rangle_N = \sum_{k_1,k_2,...,k_m} \prod \exp(\tfrac{N}{2\pi\sqrt{-1}} \pm \mathrm{Li}_2(e^{2\pi\sqrt{-1}(\frac{k_i}{N} - \frac{k_j}{N})}) + other_{n,k}) \tag{1.5}$$

$$= N^m \sum_{k_1,k_2,...,k_m} \tfrac{1}{N^m} \exp(\tfrac{N}{2\pi\sqrt{-1}} \sum \pm \mathrm{Li}_2(e^{2\pi\sqrt{-1}(\frac{k_i}{N} - \frac{k_j}{N})}) + other_{n,k}) \tag{1.6}$$

The following equlity is reasonable though there isn't mathematically rigorous proof yet .

$$\langle L\rangle_N = N^m \int_0^1 dx_1 ... \int_0^* dx_m \exp(\frac{N}{2\pi\sqrt{-1}} \sum \pm \mathrm{Li}_2(e^{2\pi\sqrt{-1}(x_i - x_j)}) + other) \tag{1.7}$$

By change of variables, put $e^{2\pi\sqrt{-1}x_i} = z_i$ and let $V(z_1, ...z_m) := \sum \pm \mathrm{Li}_2(\frac{z_i}{z_j})$

$$\langle L\rangle_N = N^m \int_{C_1} \frac{dz_1}{2\pi\sqrt{-1}z_1} ... \int_{C_m} \frac{dz_m}{2\pi\sqrt{-1}z_m} \exp(\frac{N}{2\pi\sqrt{-1}} V(z_1, ...z_m) + other) \tag{1.8}$$

By Stationary phase method, After detouring contour through the stantionary point, the integral localize on the critical point $\zeta = (\zeta_1, ...\zeta_2)$.

$$\langle L\rangle_N = N^m \frac{1}{2\pi\sqrt{-1}\zeta_1} ... \frac{1}{2\pi\sqrt{-1}\zeta_m} e^{other_\zeta} \exp(\frac{N}{2\pi\sqrt{-1}} V(\zeta_1, ...\zeta_m)) \tag{1.9}$$

Now, recall the volume conjecture,

$$2\pi \lim_{N\to\infty} \frac{\log|\langle L\rangle_N|}{N} = \mathrm{Im} V(\zeta) \tag{1.10}$$

Therefore, if one assume that all the difficult analysis problems in above equalities are totally solved then the remaining question of volume conjecture is only whether $\mathrm{Im}V(\zeta)$ is actual hyperbolic volume of L.

The answer of this questions is first appeared in the preprint [29] of Y. Yokota. In ten years later [5], J. Cho show that it holds for the complex volume of twist knot using Zickert formula[31] and Y.Yokota finished the proof in [30] for general cases but still remaining quite difficult combinatorics because of collapsing of triangulation. Finally the complicated collapsing process can be eliminated in [2]. we summarize the last result briefly.

Kashaev R-matrix has q-series $(q)_{k_i-k_j}$ terms corresponding to each corners of the diagram and index parameter k_i corresponding to each edges, so we define potential function V_D of link diagram D in the following as the summation of formally substitued Li_2 terms over all corners as in figure 1.1,

$$V_D(z_1, z_2, ...z_m) := \sum_{c \in \text{all corners}} \sigma_c \mathrm{Li}_2(\frac{T_c}{I_c}) \tag{1.11}$$

where corner sign σ_c is the rule in figure 1.2.

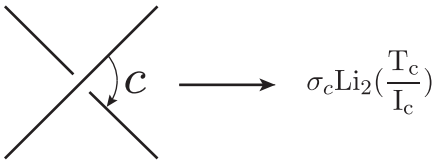

I_c : over edge of corner c
T_c : under edge of corner c
σ_c : sign of corner c

Figure 1.1: Dilogarithm terms corresponds to each corners in the diagram

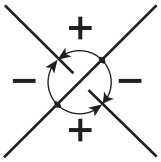

assign + to σ_c if the counter-clockwise rotation
in the corner c is from over edge to under edge .

Figure 1.2: corner sign σ_c

Then, we have the following theorem.

Theorem 1.1 (Cho-Kim-K, [2]). *A branch of V_D has $\sqrt{-1}(\mathrm{vol}(L)+\sqrt{-1}\mathrm{CS}(L))$ as the maximal critical value unless critical equations has empty solution. Moreover the valid branch of V_D is determined by $\widehat{V_D}(z_1,...,z_m) := V_D(z_1,...z_m)-\sum(\log z_i)(z_i\frac{\partial V_D}{\partial z_i})$*

1.3 Potential functions

It may be a well-known fact that hyperbolic volume is the maximize point over a certain structure deformations like Neumann-Zagier's incomplete deformation[24], but if one hope to use saddle point method to get hyperbolic volume like optimistic limit, it is difficult to adapt the above volume maximizing property since we can't say that hyperbolic volume itself is a critical value of volume functions on ambient domain containing the deformation variety.

In this chapter, we will investicate a sufficient conditioin to give the hyperbolic volume as a critical value of a function on an open domain.

1.3.1 Volume potential of dilogarithm type

Dilogarithm volume potential datum D is defined by

$$D := (\rho_k, \sigma_k, \tau_k^i, a_{ij}, b_i)$$

$$\text{with} \quad |\rho_k| = 1, \;\; \sigma_k \in \{+1,-1\}, \;\; \tau_k^i \in \{-1,0,1\}, \;\; a_{ij} = a_{ij} \in \mathbb{Z}, \;\; b_i \in \mathbb{Z},$$

where $i,j \in \{1,2,...,m\}$ is a index for complex variables and $k \in \{1,2,...,n\}$ is a index for dilogarithm terms. Let Δ_k be *simple monomial* functions of complex variables $\mathbf{z} = (z_1, z_2, ..., z_n)$ which means that can be written in the following expressions,

$$\Delta_k = \rho_k z_1^{\tau_k^1} z_2^{\tau_k^2} \cdots z_n^{\tau_k^n} \quad \text{with} \;\; \tau_k^i \in \{+1,\ 0,\ -1\} \tag{1.12}$$

And *dilogarithm volume potential function* V_D for the given potential datum D is defined by

$$V_D(z_1,...,z_n) = \sum_k \sigma_k \mathrm{Li}_2(\Delta_k^{\sigma_k}) + \sum_{i,j} \frac{1}{2} a_{ij} \log z_i \log z_j + \sum_i \sqrt{-1} b_i \log z_i \tag{1.13}$$

1.3.2 Critical equations

Definition 1.2. A system of *critical equations* $\mathcal{C}_D$ is defined by

$$\mathcal{C}_D = \left\{ \exp(z_i \frac{\partial V_D}{\partial z_i}) = 1 \,\middle|\, i = 1,2,...,n \right\}. \tag{1.14}$$

Definition 1.3. A *compensated evaluation* $\widehat{V}_D$ is defined by

$$\widehat{V}_D(\mathbf{z}) = V_D(\mathbf{z}) - \sum_i (\log z_i)(z_i \frac{\partial V_D(\mathbf{z})}{\partial z_i}). \tag{1.15}$$

Let $\mathcal{S}_D$ be the solution set of $\mathcal{C}_D$. we can easily observe that $\mathcal{C}_D$ consists of rational equations of complex parameter z_i's. In fact, above several definitions are devised to hold the following properties.

Lemma 1.4 ([2])**.** *$\widehat{V}_D$ is independant of branch choices and locally constant on $\mathcal{S}_D$.*

Proof. Proof is same with lemma 2.1 and 2.2 in [2]. The other way to see this lemma is that it is a corollay of theorem 1.8. □

Theorem 1.5. *The evalutations of $\widehat{V}_D$ on the $\mathcal{S}_D$ is just the summation of Bloch-Wigner functions of Δ_k's, i.e,*

$$\mathrm{Im}\widehat{V}_D = \sum D(\Delta_k). \tag{1.16}$$

Proof.

$$z_i \frac{\partial \mathrm{Li}_2(\Delta_k^{\sigma_k})}{\partial z_i} = -\sigma_k \tau_k^i \log(1 - \Delta_k^{\sigma_k}) \tag{1.17}$$

$$0 = \mathrm{Re}(z_i \frac{\partial V}{\partial z_i}) = -\sum_k \sigma_k \tau_k^i \log|1 - \Delta_k^{\sigma_k}| + \sum_j a_{ij} \log|z_j| \tag{1.18}$$

$$\begin{aligned}
\mathrm{Im}\,\widehat{V}_D &= \sum_k \sigma_k \mathrm{Im}\,\mathrm{Li}_2\,({\Delta_k}^{\sigma_k}) + \sum_{k,i} \sigma_k \tau_k^i \mathrm{Im}\,(\log z_i \log(1 - {\Delta_k}^{\sigma_k})) \\
&\quad - \sum_{i,j} \frac{1}{2} a_{ij} \mathrm{Im}\,(\log z_i \log z_j) \\
&= \sum_k \sigma_k D(\Delta_k^{\sigma_k}) - \sum_k \sigma_k \arg(1 - \Delta_k^{\sigma_k}) \log|\Delta_k^{\sigma_k}| \\
&\quad + \sum_{k,i} \sigma_k \tau_k^i \arg z_i \log|1 - \Delta_k^{\sigma_k}| + \sum_{k,i} \sigma_k \tau_k^i \log|z_i| \arg(1 - \Delta_k^{\sigma_k}) \\
&\quad - \sum_{i,j} \frac{1}{2} a_{ij} \log|z_i| \arg z_j - \sum_{i,j} \frac{1}{2} a_{ij} \arg z_i \log|z_j| \\
&= \sum_k \sigma_k D(\Delta_k^{\sigma_k}) + \sum_i \arg z_i \left(\sum_k \sigma_k \tau_k^i \log|1 - \Delta_k^{\sigma_k}| - \sum_j a_{ij} \log|z_j| \right)
\end{aligned}$$

By (1.18), we can observe the remaining terms cancle out over the critical set $\mathcal{S}$ and the imaginary part of the evaluation of $\widehat{V}_D$ give nothing other than the summation over *Bloch-Wigner* functions of Δ_k's.

$$\operatorname{Im}\widehat{V}_D\Big|_{\mathbf{z}=\zeta} = \sum_k \sigma_k D(\Delta_k^{\sigma_k}) = \sum_k D(\Delta_k) \qquad \text{for} \quad \zeta \in \mathcal{S}. \tag{1.19}$$

□

Corollary 1.6. *Suppose that hyperbolic manifold M is given by an algebraic sum of ideal tetrahedra which is paramaterized by simple monomials and it's critical equation satisfy the system of Thurston gluing equations, then the imaginary part of $\widehat{V}_D$ of a solution ζ is the hyperbolic volume of the representation induced by ζ.*

Remark 1.7. we can expect that $\widehat{V}_D$ give whole complex volume [2],[3],[30], but It's false in general. There is s subtle issue for potential function to produce the accurate Chern-Simons invariants modula π^2, not $\pi^2/6$.

In this article we will only focus on the hyperbolc volume not Chern-Simons invariant, i.e, imaginary part of $\widehat{V}_D$. Since for manifolds with totally geodesic boundars, it is not clear at present the right definition of Chern-Simons invariants for the manifold with geodesic boundaries.

1.3.3 Analytic continuation $\widetilde{V}_D$ and compensated evaluation $\widehat{V}_D$

Finally, let us see the role of compensated evaluation $\widehat{V}_D$. Recall $\widetilde{V}_D$ means an analytic continuation of V_D hence we should choose a correct brach to obtain a correct value $\widetilde{V}_D(\widetilde{z})$. Branch problem is not so easy in general but we have an easy solution for correct branch choice in our cases.

Theorem 1.8. *Let V be a dilogarithm type potential function and suppose that $\widetilde{z}$ is a critical point of $\widetilde{V}$. Then we have*

$$\widetilde{V}(\widetilde{z}) \equiv \widehat{V}(z) \mod \pi^2 \tag{1.20}$$

Proof. Recall the general form in 0.2 of an arbitrary dilogarithm branch.

$$\begin{aligned}\widetilde{V}(\widetilde{z}) &= \sum_k \sigma_k \widetilde{\mathrm{Li}_2}(\widetilde{\Delta_k^{\sigma_k}}) + \sum_{i,j} \frac{1}{2} a_{ij} \widetilde{\log} \widetilde{z_i} \widetilde{\log} \widetilde{z_j} + \sum_i \sqrt{-1} b_i \widetilde{\log} \widetilde{z_i} \\ &\equiv \sum_k \sigma_k \mathrm{Li}_2{}^*(\Delta_k^{\sigma_k}) + \sum_k 2w_k \pi \sqrt{-1} \log^*(\Delta_k^{\sigma_k}) \\ &\quad + \sum_{i,j} \frac{1}{2} a_{ij} \log^* z_i \log^* z_j + \sum_{i,j} \pi a_{ij} w_i \sqrt{-1} \log^* z_i \\ &\quad + \sum_i \sqrt{-1} b_i \log^* z_i \mod \pi^2 \end{aligned} \tag{1.21}$$

where w_i and w_k are winding numbers of a contour of $\widetilde{z}$ of z_i and $\Delta_k^{\sigma_k}$, repectively. Since $\widetilde{z}$ is a critical point of $\widetilde{V}$ we have

$$\begin{aligned} z_i \frac{\widetilde{V}}{z_i} &= \sum_k -\sigma_k \sigma_k \tau_k^i \log^*(1 - \Delta_k^{\sigma_k}) + \sum_k 2w_k \pi \sqrt{-1} \sigma_k \tau_k^i \\ &\quad + \sum_j a_{ij} \log^* z_j + \sum_j 2\pi a_{ij} w_i \sqrt{-1} \\ &\quad + \sqrt{-1} b_i = 0. \end{aligned} \tag{1.22}$$

As combining 1.21 and 1.22, we conclude

$$\begin{aligned} \widetilde{V}(\widetilde{z}) &= V^*(z) - \sum_i (\log^* z_i)(z_i \frac{\partial V^*(z)}{\partial z_i}) \\ &= V(z) - \sum_i (\log z_i)(z_i \frac{\partial V(z)}{\partial z_i}). \end{aligned}$$

□

Chapter 2

Knotted graph complements

2.1 Hyperbolic structure for complements

We want to define a proper hyperbolic structure of knotted graph complemts. At first, we can consider usual open tubular neighborhood complement $S^3 \setminus N(G)$, it is topological manifold with boundaries. If one assume the complementary space have hyperbolic structure with totally geodesic boundary then we can find out rigidity property immediately by double of the manifold. Hence we can expect for hyperbolic volume to be knotted graph invariant.

But this definition is not so quite satisfactory because **I-H** move or merging vertices preserve topological complementary space. $S^3 \setminus N(G)$ is nothing but knotted bouquet for all knotted graph G.

For more proper invariant for knotted graph, we consider pared manifold(see [12], [13]) structure which is a certain type of hyperbolic manifolds with totally geodesic

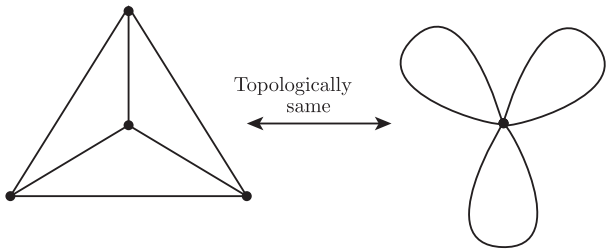

Figure 2.1: Tetrahedron graph vs bouquet with 3-leaves

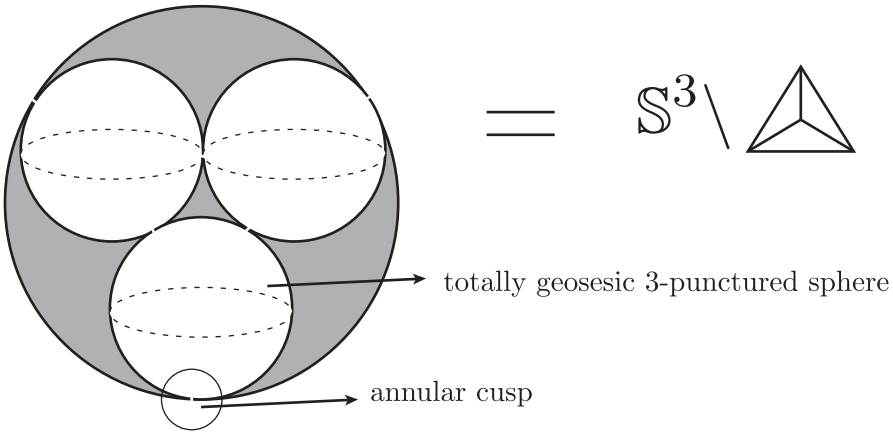

Figure 2.2: hyperbolic structure for the teterahedron graph complement

boundary and annular cusp. we add the condition that the meridians of every edges in the graph give parabolic elements in $PSL(2,\mathbb{C})$ by the holonomies.

Definition 2.1 (knotted graph complement)**.** A knotted graph complement M_G is a topologically complementary space of union of the graph and open neighborhood of the vertices.

$$M_G := S^3 \setminus \{G \bigcup N(v(G))]\} \tag{2.1}$$

If M_G allow complete hyperbolic structure with totally geodesic boundaries, every edge meridian holonomy should be parabolic elements and every vertices correspond $\deg(v)$-punctured hyperbolic spheres. This hyperbolic structure is better invariant than the previous genuine complement of the knotted graph. In fact quiet many knotted graph can be distinguished via their hyperbolic structure like knot complements case. In this paper, we always assume hyperbolic graph without a mention and the final goal is to construct volume potential function giving hyperbolic volume of the graph.

2.2 Ideal triangulations

This triangulation of knotted graph is originated from octahedral decomposition of link complements. The octahedral decomposition have been used in several litera-

tures [28],[30]. In pariticular, A triangulation not eliminating additional two points was used in [2].

Similarily, instead of $M_G := S^3 \setminus \{G \bigcup N(v(G))\}$, we triangulate $M_G \setminus \{+\infty, -\infty\}$ where $+\infty, -\infty$ are additional two points. Because their fundamental groups are same, M_G and $M_G\{+\infty, -\infty\}$ has same represenations into $PSL(2, \mathbb{C})$. Note that

$$\begin{aligned} M_G \setminus \{+\infty, -\infty\} = & \quad S^3 \setminus \{G \bigcup N(v(G) \bigcup \{+\infty, -\infty\}\} \\ = & \quad S^2 \times (0,1) \setminus \{G \bigcup N(v(G))\}. \end{aligned}$$

We will decompose $S^2 \times (0,1)$ considering $S^2 \times \frac{1}{2}$ is the plane on which the knotted graph diagram drawn.

2.2.1 Dual graph decomposition for diagram

Consider a dual graph of the given knotted graph diagram, then their faces contain only one vertex or one crossing of the original diagram. we will construct unit blocks corresponding to each faces in the dual graph diagram as in figure 2.4.

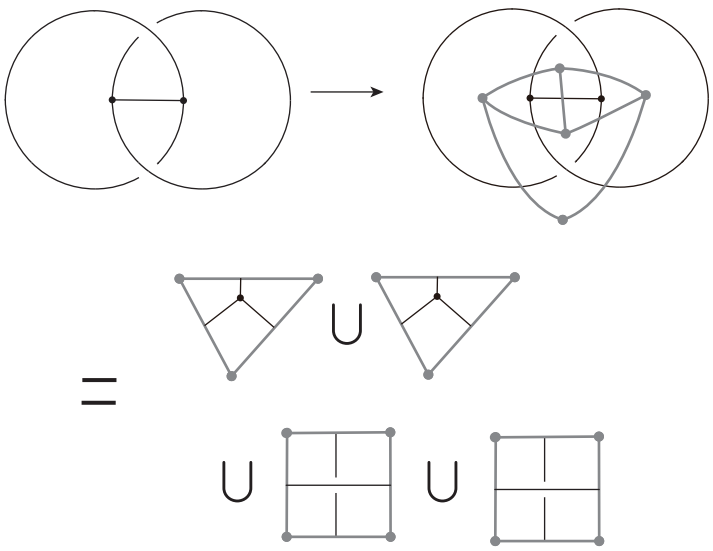

Figure 2.3: Dual graph decomposition for knotted graph diagram

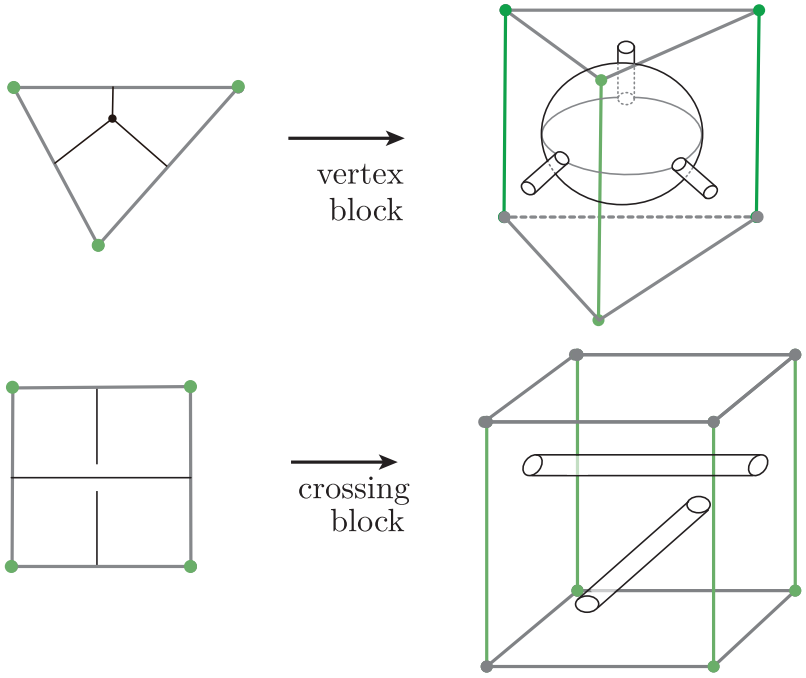

Figure 2.4: Each face of dual graph correspond unit blocks

We can observe that the unit blocks can be decomposed into ideal tetrahdra whose vertices indicate $\pm\infty$ points and edges of the graph which is a cusp point of M_G as like the following figure 2.6 and 2.5. We call this cell decomposition of M_G as *generalized octahedral decomposition* and denotes the triangulation by $\mathcal{T}_G$.

We should note that an octahedron can be decompose into four tetrahedra by canonical way where each tetrahedron is obtained by join of central 1-cell and horizontal 1-cell. For example, central 1-cell δ and horizontal 1-cell γ_{ab} make a tetrahedra with six 1-cells of α_a, β_a, α_b, β_b, γ_{ab}, δ.

Remark 2.2. This decomposition of an octahedron is called 4-term decomposition. four-term decomposition is closely related to Kashaev R-matrix. Meanwhile each entry of colored Jones R-matrix consist of five quantum factorial term. this is related to five-term decomposition of an octahedron. For more detail about this topic, see [3],[4].

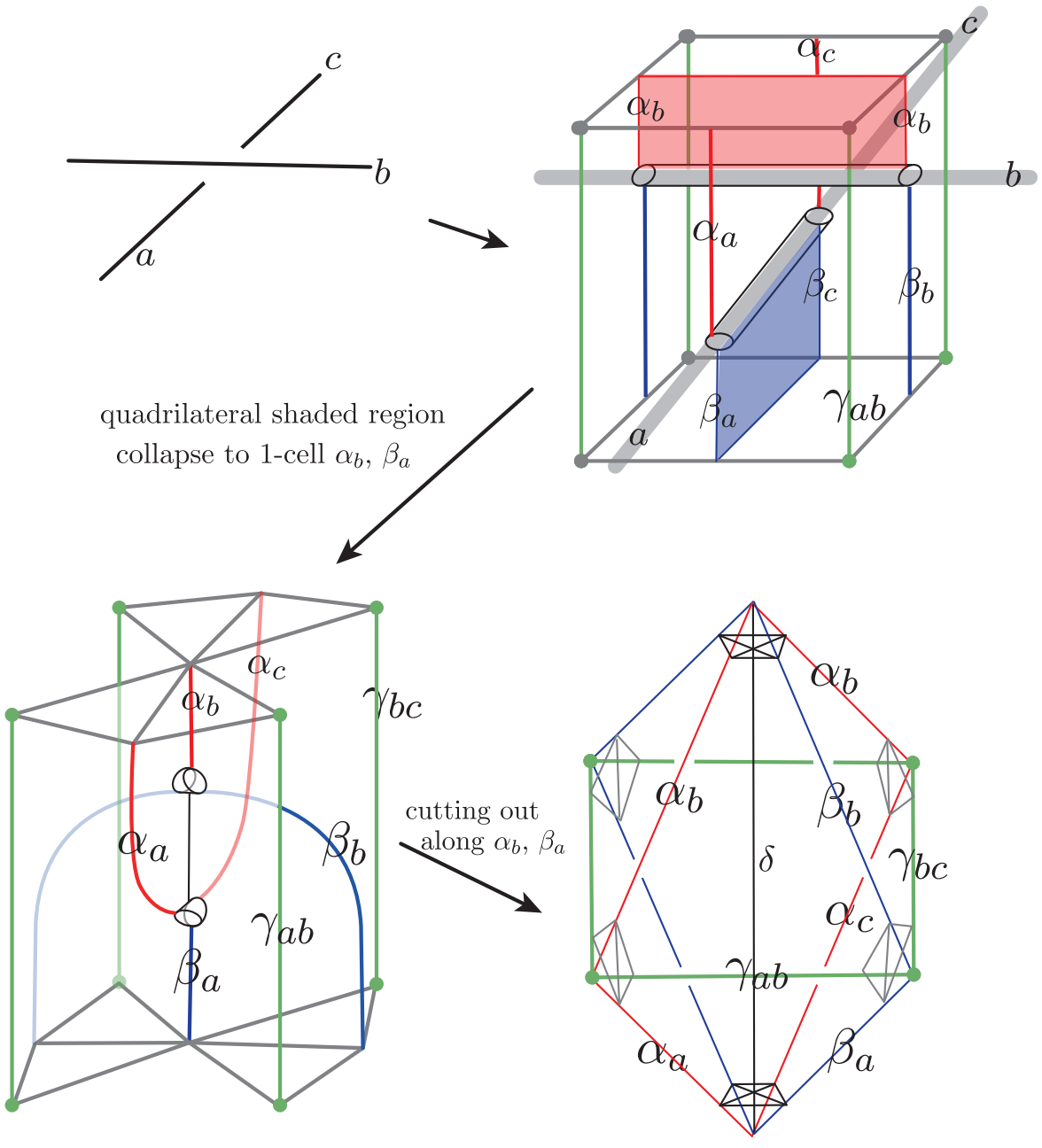

Figure 2.5: Decomposition of crossing block

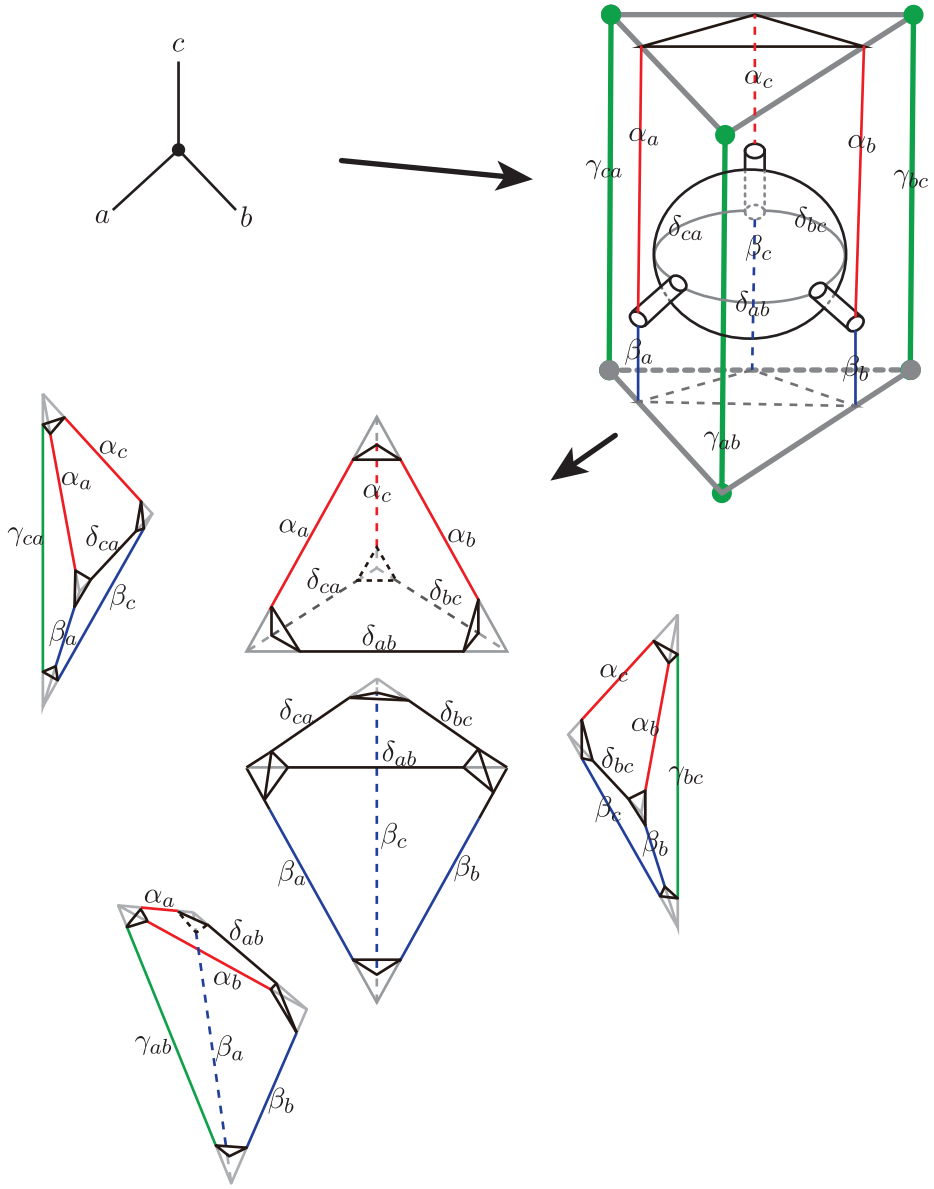

Figure 2.6: Decomposition of vertex block

2.2.2 Combinatorial features: 1-cell

Let us consider figure 2.5 and 2.6. As the figures, we classify every 1-cells in the triangulation as the followings,

- α edge is an 1-cell in $\mathcal{T}_G$ joing $+\infty$ point and a graph point
- β edge is an 1-cell in $\mathcal{T}_G$ joing $-\infty$ point and a graph point
- γ edge is an 1-cell in $\mathcal{T}_G$ joing $-\infty$ point and $+\infty$ point.
- δ edge is an 1-cell in $\mathcal{T}_G$ joing two points in edges of graph.

and draw this edges directly on the dual grah decomposition diagram.

Example 2.3. *Consider graph diagram in figure2.3, we can draw as the following figure 2.7.*

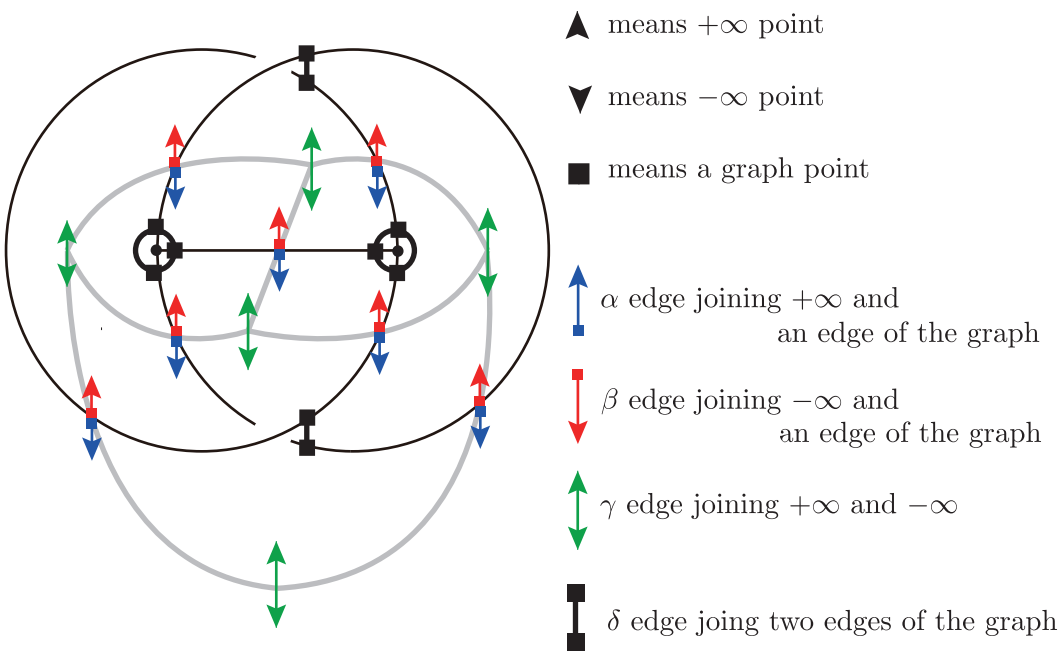

Figure 2.7: 1-cell structure of $\mathcal{T}_G$ which is drawn on the graph diagram.

We can easily check the following lemma.

Lemma 2.4. *All α edges(or β edges) on the same over-bridge(or under-bridge, repectively) in the diagram are identified into an one-cell in $\mathcal{T}_G$*

Proof. Considering figure 2.5, β_a edge and β_b edge should be identified into one 1-cell. Similarily all α edges (or β edges) over the same over-bridge (or under-bridge, repectively) should be identified into one 1-cell. □

Proposition 2.5. *We can enumerate 1-cells of $\mathcal{T}_G$ by read off bridges,segments, regions and crossings of the diagram.*

- *α edge corresponds over-bridge and under-segment of arcs of the diagram.*
- *β edge corresponds under-bridge and over-segment of arcs of the diagram.*
- *γ edge corresponds regions(2-faces) in the graph diagram.*
- *δ edge corresponds crossing points and coners of vertices.*

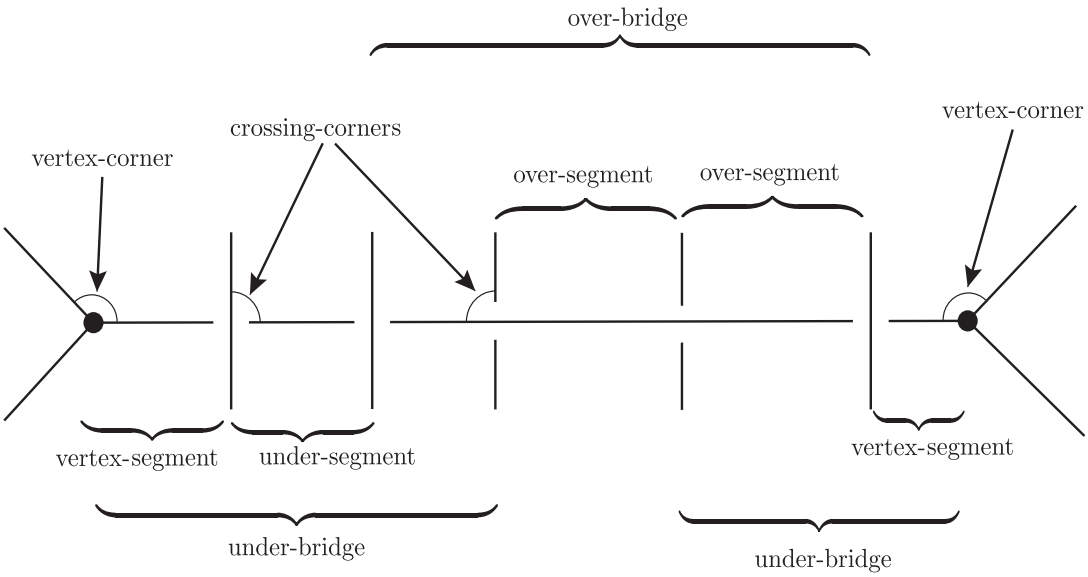

Figure 2.8: bridges, segments and corners in diagrm

2.2.3 Combinatorial features: 3-cell

We note that each corner of original graph diagram meets exactly 6 edges consisted of two α edges, two β edges, a γ edge, a δ edge. Therefore we can realize each corner indicate exactly one 3-simplex in the triangulation as comparing each piece of a unit block in figure 2.5, 2.6 and each corner of diagram 2.7.

Moreover we can also classify whole 3-cells in $\mathcal{T}_G$ into the following three types.

- crossing-corner tetrahedron like in figure 2.9
- vertex-corner tetrahedron like in 2.10
- upper-pyramid and lower pyramid like in 2.10

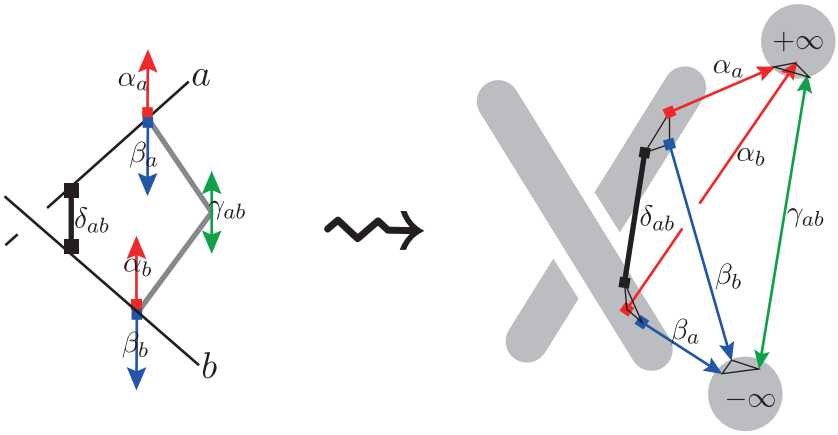

Figure 2.9: crossing-corner tetrahedron

The orientation of crossing corner tetrahedra is a little confusing. At that time, we can refer the original octahedron figure 2.5 and choose the right orientation. We can easily observed that the number of corner tetrahedra is the number of corners in the diagram and the number of upper- or lower- pyramid is the number of vertices in the diagram.

The following arguments says that upper- and lower pyramids are determined up to hyperbolic isometry from the shape parameters of corner tetrahera. So we don't need to consider these pyramids to investigate hyperbolic structure of a hyperbolic knotted graph complement.

Lemma 2.6. *The upper pyramid and lower pyramid can be glued into bi-pyramid.*

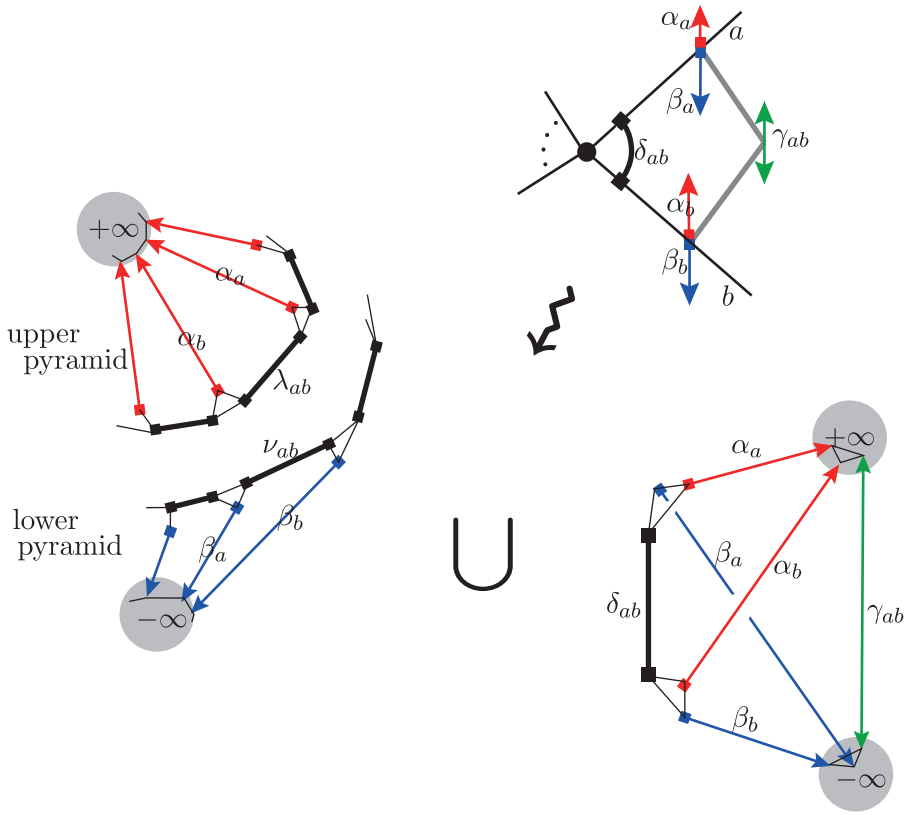

Figure 2.10: upper-, lower-pyramid and vertex-corner tetrahedron

Proof. Since we assume hyperbolic graph, bottom faces of upper- and lower- pyramids of same vertex are glued into totally geodesic $\deg(v)$-puntured sphere. We can develope the punctured sphere on the poincare disk and observe that identified by an inversion on the disk. It means that bottom faces of the pyramids can be identified by orientation preserving isometry of hyperbolic 3-space. □

We can give a complex parameter to each horizontal edges of hyperbolic ideal bi-pyramid by taking a cross-ratio

$$[\textit{upper-vertex} : \textit{lower-vertex} : \textit{initial-vertex} : \textit{terminal-vertex}]$$

where initial- or terminal vertex is determined after fixing an orientation of the horizontal edge.

Remark 2.7. In fact, we can define complex shape parameters for all edges of a convex polyhedron with triangular faces taking similar cross-ratio. It is obvious fact that if two hyperbolic ideal convex polyhedra have same edge parameters, then these are congruent up to hyperbolic isometry.

Lemma 2.8. *Hyperbolic ideal bi-pyramid is uniquely determined by the shape parameters of horizontal edges*

Proof. The complex parameters of the other 1-cells of bi-pyramid are determined by only horizontal edges. □

We note that 1-cell of these bipyramids consist of α edges and β edges and horizontal edges. In particular, the horizontal edges are identified δ edges in $\mathcal{T}_G$ and each horizontal edge of pyramids is refered by a corner of diagram.

Suppose a corner be placed between segment a and b, the corner is denoted by two segment a and b. A horizontal edge of upper pyramid or under-pyramid is denoted by λ_{ab} or ν_{ab}.

Proposition 2.9. *Upper- and lower- pyramid is determined by the corner tetrahedrons.*

Proof. It should be noted that

$$\nu_{ab}\lambda_{ab}\delta_{ab} = -1 \tag{2.2}$$

since those 1-cells identified into same edge of boundary punctured sphere and the total angle summation is π. A horizontal edge of a bi-pyramid have the shape parameter $\nu_{ab}\lambda_{ab} = \frac{-1}{\delta_a b}$. By lemma 2.8, we can get bi-pyramid and recover the upper- and lower- pyramid by cutting out hyrizontal faces. □

Remark 2.10. In fact, there are subtle issue to cut out bi-pyramid into two pyramid. If you assume genuine hyperbolic structure, then you meet no problem. But you have whole corner tetrahedra given by only shape parameters, you should check that it is possible to make a punctured-sphere.

Remark 2.11. From the point of view of $PSL(2,\mathbb{C})$-representation, The shape parameters satisfying Thurston gluing equations give a representation from *twisted double* of the graph complement into $PSL(2,\mathbb{C})$. Moreover, discrete faithful representation of the twisted double of a graph complement produce a hyperbolic cusped manifold which is scissors congruent to two times of the hyperbolic graph complement. The detailed treatment for twisted double of knotted graph complement will be appeared in succeding papers.

2.3 Edge parametrization

To avoid confusing, we need to define more notations. As the before, γ edges in $\mathcal{T}_G$ have one to one correspondence to regions of the diagram. We denote γ edge representing a region r by γ_r.

A 3-cell which meets γ_r is exactly representated by a corner of the graph diagram. Every corner meet two adjacent segments and one vertex(or crossing) and one region we can denote corners by two segments or adjacent vertex and region.

Let a, b be segments and r be a region. Let v be a vertex or a crossing. We denote one corner of diagram by ab or rv. So γ_{ab} or γ_{rv} means an 1-cell which glued $gamma_r$ in 3-simplex represented by the corner ab or rv.

We can express edge equation as the following.

$$\text{edge gluing equation of } \delta_r = \prod_{r\sim v} \delta_{rv} \tag{2.3}$$

If we put the shape parameter of this simplex as the counter clockwise ratio of incident segments, then equation 2.3 hold automatically. and δ_{ab} is dual of γ_{ab} and has same shape parameter. Hence for a crossing x, δ_x edge equation also hols.

In knot complement cases, this parametrization truely works well(see [2] for detail), but the graph comement cases cause some troubles. This problem comes the following observation. Recall the fact that each δ edge is contained in geodesic boundary and

$$\delta_{ab}\delta_{bc}\delta_{ca} = -1 \tag{2.4}$$

Note the figure 2.6, 2.10 and

$$\delta_{xy} = \lambda_{xy}\nu_{xy}\frac{x}{y}$$

where λ and ν is upper pyramid and lower pyramid, respectively in figure 2.6. Therefore as combining above two indentity, we have

$$\delta_{ab}\delta_{bc}\delta_{ca} = \frac{a}{b}\lambda_{ab}\nu_{ab}\frac{b}{c}\lambda'_{ab}\nu'_{ab}\frac{c}{a}\lambda''_{ab}\nu''_{ab} = 1. \tag{2.5}$$

This contradicts to equation 2.4.

2.3.1 Corner parity system

This parametrization works well for knot or link diagram case, but unfortunately, it always derived contradition for the graph diagram. To overcome this problem, we can define corner parity system.

Definition 2.12. Corner parity system $\mathcal{P}_G$ for a plane diagram is defined by a function satisfying the following two properties.

$$\mathcal{P}_G : \mathcal{C} \longrightarrow \{+1, -1\} \tag{2.6}$$

where $\mathcal{C}$ the set of all coners of the diagram.

$$1) \quad \prod_{c \text{ meets } v} \mathcal{P}_G(c) = \quad (-1)^{\deg v} \quad \text{for all vertex } v \in G \tag{2.7}$$

$$2) \quad \prod_{c \text{ meets } f} \mathcal{P}_G(c) = \quad 1 \quad \text{for all faces } f \in G \tag{2.8}$$

If every corner have $+1$ or -1 satisfying above two property, We can take the shape parameter of corner ab as the following.

$$\mathcal{P}_G(ab)\frac{a}{b}. \tag{2.9}$$

Then we can avoid the contradiction like 2.5. For this strategy, the following theorems arise naturally.

Theorem 2.13. *For every plane graph G, corner parity system $\mathcal{P}$ exists always.*

Definition 2.14. edge parity system $\mathcal{E}_G$ for a plane diagram G is defined by a function

$$\mathscr{E}_G : \mathcal{E} \longrightarrow \{+1, -1\} \tag{2.10}$$

Theorem 2.15. *Let $\mathcal{P}_1$ and $\mathcal{P}_2$ be two different corner parity systems for the same diagram G. There exist an edge parity $\mathscr{E}$ which transit from $\mathcal{P}_1$ to $\mathcal{P}_2$ by the action $\mathcal{E} \cdot \mathcal{C}$. Moreover this transition always preseve corner shape parameters.*

To prove above two theorems, we need some preperation. After investigating a general theory on corner chan complex, we can show these claims should be true in the obvious way.

Chapter 3

Corner chain complex

We can naturally define a certain type of chain complexes which involve so-called the corners of the graph diagram. Although the key contents are just simple combinatorics and elementary homological algebra, these materials give quite clear statements related to the corner parity system mentioned in the previous chapter and the edge parameterization for octahedral decomposition of knot or knotted graph compliments. In this chapter we don't consider knottedness and assume that all knotted crossing points of the diagram are flattened and regarded as usual 4-valent vertices.

This topic has quite a different flavor from the main subject, but the concept of those may seem to be interesting itself independently. This chapter will be treated in self-contained manners as possible and require no preliminary knowledge except cellular homology theory which is covered by any graduate textbook on algebraic topology like [11]. If you are barely familiar to graph theory and need to know the basic, any introductory article or textbook on graph is sufficient, especially survey article [1] are recommended.

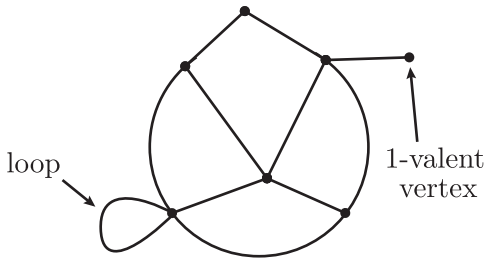

Figure 3.1: Example for a loop and an 1-valent vertex

In this chapter, we always assume that every graph has only finite vertices ,no loops (or self-loop) and no 1-valent (or degree one) vertices like figure 3.1.

3.1 Chain complexes from graphs

Let G be a connected graph diagram on the plane. Let us consider CW-complex structure $\mathcal{C}(G)$ from the plane diagram G and identify the underlying plane as 2-dimensional sphere S^2 by one-point compactification. This chain complex is easily generated by the set of vertices $V(G)$, edges $E(G)$ and faces $F(G)$, which generate free $\mathbb{Z}$-modules $\mathcal{C}_0(G)$, $\mathcal{C}_1(G)$ and $\mathcal{C}_2(G)$ respectively.

$$\mathcal{C}(G) \quad : \quad 0 \longrightarrow \mathcal{C}_2(G) \xrightarrow{d_2} \mathcal{C}_1(G) \xrightarrow{d_1} \mathcal{C}_0(G) \longrightarrow 0$$

As considering directed graph, we can determine boundary homomorphism d_k canonically from the direction of edges. The reduced homology group with augmentation vanish except 2-dimensional fundamental cycle, since the underlying space is nothing but S^2. If one attaches additional modules $\ker d_2$ at the higher degree, we have $\widetilde{\mathcal{C}(G)}$, an exact sequence (or an acyclic chain complex), called as *diagram exact sequence* or *diagram chain complex* of G

$$\widetilde{\mathcal{C}(G)} \quad : \quad 0 \longrightarrow \ker d_2 \xhookrightarrow{\iota} \mathcal{C}_2(G) \xrightarrow{d_2} \mathcal{C}_1(G) \xrightarrow{d_1} \mathcal{C}_0(G) \xrightarrow{\epsilon} \mathbb{Z} \longrightarrow 0$$

It is possible to consider the case of G embedded in an arbitrary surface. We note that the embedding of G should be *cellular* (see [1]) for the diagram sequence to be CW-complex. This chain complex is nothing other than CW-complex of the underlying surface.

3.2 Corner homormorphisms

3.2.1 Corners and the incident maps

Definition 3.1. A *corner* of G means the intersection between a small neighborhood of a vertex v and a face f only if v and f are incident, denoted by $\mathrm{c}(v, f)$. And the set of corner of G is denoted by $C(G)$.

If one takes a corner x, there are exactly one vertex, one face and two edges which are incident to the corner x. Since G doesn't allow loops and 1-valent vertices, it is obvious that every corner of G has exactly two different incident edges. It is

convenient to consider these things as maps on $C(G)$, i.e. V_x, F_x, I_x and T_x denote the vertex, the face, the initial edge and the terminal edge of the corner x, respectively.

The choice of the initial or terminal edge comes from that the rotational direction at the incident vertex is counter-clockwise from the initial edge to the terminal edge, i.e. agree with the standard orientation of the plane on which the diagram G is drawn.

Definition 3.2. The followings are called *incident maps* defined on $C(G)$

$$\begin{aligned} V: &\quad C(G) \longrightarrow V(G) \quad \text{by} \quad x \longmapsto V_x \\ F: &\quad C(G) \longrightarrow F(G) \quad \text{by} \quad x \longmapsto F_x \\ I: &\quad C(G) \longrightarrow E(G) \quad \text{by} \quad x \longmapsto I_x \\ T: &\quad C(G) \longrightarrow E(G) \quad \text{by} \quad x \longmapsto T_x \end{aligned}$$

For example, if one takes $x := c(v, f)$, i.e. the corner x is indicated by a vertex v and a face f then V_x and F_x denote the vertex v and the face f respectively, as in figure 3.2

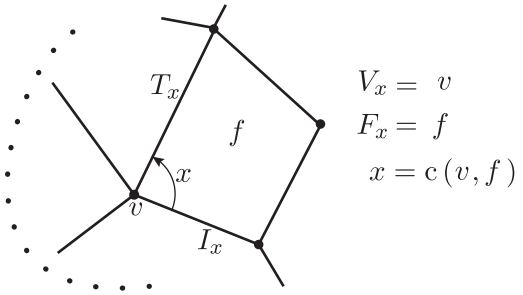

Figure 3.2: V_x, F_x, I_x and T_x are incident to a corner x

Definition 3.3. Let us define convenient notations to refer to the incident relations between a corner and the others as the followings.

$$\begin{aligned} c \overset{V}{\curvearrowright} v \quad \text{or} \quad v \overset{V}{\curvearrowleft} c &\overset{def}{\Longleftrightarrow} v = V_c \\ c \overset{E}{\curvearrowright} f \quad \text{or} \quad f \overset{E}{\curvearrowleft} c &\overset{def}{\Longleftrightarrow} f = F_c \\ c \overset{T}{\curvearrowright} e \quad \text{or} \quad e \overset{T}{\curvearrowleft} c &\overset{def}{\Longleftrightarrow} e = T_c \\ c \overset{I}{\curvearrowright} e \quad \text{or} \quad e \overset{I}{\curvearrowleft} c &\overset{def}{\Longleftrightarrow} e = I_c \end{aligned}$$

and $x \sim y$ are also convenient, means that x and y are incident, i.e. $x \overset{V}{\sim} y$ or $x \overset{E}{\sim} y$ or $x \overset{T}{\sim} y$ or $x \overset{L}{\sim} y$.

Definition 3.4. Moreover, we can define another notation for an incident relation of edges sharing a common corner unless the edges produce a bigon like figure 3.3.

$$e_i \to e_j \quad \text{or} \quad e_j \leftarrow e_i \overset{def}{\Longleftrightarrow} e_i = I_c \text{ and } e_j = T_c \text{ for a corner } c$$

3.2.2 $\mathscr{C}, \mathscr{E}$, $\mathscr{VF}$ and homomorphisms

Let $\mathscr{C}$, $\mathscr{E}$ and $\mathscr{VF}$ be free $\mathbb{Z}$-modules generated by $C(G)$, $E(G)$ and $V(G) \cup F(G)$, respectively. And let us define *corner homomorphisms* by using incident maps.

Definition 3.5. Let $\mathbb{Z}$-module homomorphisms $\boldsymbol{ce}$ and $\boldsymbol{cvf}$ be defined by the followings

$$\begin{aligned} \boldsymbol{ce} &: \mathscr{C} \longrightarrow \mathscr{E} \quad \text{by} \quad x \longmapsto T_x - I_x, \quad x \in C(G) \\ \boldsymbol{cvf} &: \mathscr{C} \longrightarrow \mathscr{VF} \quad \text{by} \quad x \longmapsto V_x - F_x, \quad x \in C(G) \end{aligned}$$

And we define a kind of structure constant of the corners of the graph, just imitating Kronecker delta δ.

Definition 3.6. Let *corner incident delta* δ_{xy} or $\delta(x, y)$ be defined by the following.

$$\delta_{xy} = \begin{cases} 1 & \text{if} \quad x \overset{V}{\sim} y \text{ or } x \overset{T}{\sim} y \\ -1 & \text{if} \quad x \overset{E}{\sim} y \text{ or } x \overset{L}{\sim} y \\ 0 & \text{otherwise} \end{cases}$$

From the above definitions, we have following formulas.

Proposition 3.7.

$$\begin{aligned} \boldsymbol{cvf}\left(\sum_{c \in C(G)} a_c c\right) &= \sum_{v \in V(G)} \left(\sum_{c \in C(G)} \delta_{cv} a_c\right) v + \sum_{f \in F(G)} \left(\sum_{c \in C(G)} \delta_{cf} a_c\right) f \\ \boldsymbol{ce}\left(\sum_{c \in C(G)} a_c c\right) &= \sum_{e \in E(G)} \left(\sum_{c \in C(G)} \delta_{ce} a_c\right) e \end{aligned}$$

where a_c is some $\mathbb{Z}$-coefficients in $\mathscr{C}$.

Consider dual mappings $\boldsymbol{ce}^* : \mathscr{E}^* \longrightarrow \mathscr{C}^*$ and $\boldsymbol{cvf}^* : \mathscr{VF}^* \longrightarrow \mathscr{C}^*$ and identify $\mathscr{C}, \mathscr{E}$ and $\mathscr{VF}$ and their dual modules $\mathscr{C}^*, \mathscr{E}^*$ and $\mathscr{VF}^*$ by canonical pairing using Kronecker δ. And then we get the following additional homomorphisms.

Definition 3.8. Let $\mathbb{Z}$-module homomorphisms $\boldsymbol{ec} : \mathscr{E} \longrightarrow \mathscr{C}$ and $\boldsymbol{vfc} : \mathscr{VF} \longrightarrow \mathscr{C}$ be defined by the following commutative diagrams.

$$\begin{array}{ccc} \mathscr{E}^* & \xrightarrow{\boldsymbol{ce}^*} & \mathscr{C}^* \\ \big| \wr & & \big| \wr \\ \mathscr{E} & \xrightarrow{\boldsymbol{ec}} & \mathscr{C} \end{array} \qquad \begin{array}{ccc} \mathscr{VF}^* & \xrightarrow{\boldsymbol{cvf}^*} & \mathscr{C}^* \\ \big| \wr & & \big| \wr \\ \mathscr{VF} & \xrightarrow{\boldsymbol{vfc}} & \mathscr{C} \end{array}$$

In fact, $\boldsymbol{ec}$ and $\boldsymbol{vfc}$ are nothing but transposes of $\boldsymbol{ce}$ and $\boldsymbol{cvf}$. So we have the following formulas for $\boldsymbol{ec}$ and $\boldsymbol{vfc}$.

Proposition 3.9.

$$\boldsymbol{vfc}\left(\sum_{v\in V(G)} a_v v + \sum_{f\in F(G)} a_f f\right) = \sum_{c\in C(G)} \left(\sum_{v\in V(G)} \delta_{vc} a_v c + \sum_{f\in F(G)} \delta_{fv} a_f\right)$$

$$\boldsymbol{ec}\left(\sum_{e\in E(G)} a_e e\right) = \sum_{c\in C(G)} \left(\sum_{e\in E(G)} \delta_{ec} a_e\right) c$$

where a_v, a_f and a_e are some $\mathbb{Z}$-coefficients in $\mathscr{VF}$ and $\mathscr{E}$.

And another following formula for $\boldsymbol{vfc}$ is also useful.

Proposition 3.10.

$$\boldsymbol{vfc}\left(\sum_{v\in V(G)} a_v v + \sum_{f\in F(G)} a_f f\right) = \sum_{\substack{v\in V(G)\\ f\in F(G)}} (a_v - a_f) c(v,f) \tag{3.1}$$

where $c(v,f)$ corresponds the identity element in $\mathscr{C}$ unless v and f are incident.

Proof. Note that

$$\delta(x, c(v,f)) = \begin{cases} 1 & \text{if} \quad x = v \\ -1 & \text{if} \quad x = f \\ 0 & \text{otherwise.} \end{cases}$$

Therefore,

$$\sum_{c\in C(G)}\left(\sum_{v\in V(G)}\delta_{vc}a_v+\sum_{f\in F(G)}\delta_{fv}a_f\right)c=\sum_{\substack{v\in V(G)\\ f\in F(G)}}\left(\delta_{v,c(v,f)}a_v-\delta_{f,c(v,f)}a_f\right)c(v,f)$$

is followed by the proof. □

We would like to use a similar formula for $\boldsymbol{ec}$ using $c(e_i,e_j)$ like above (3.1), but we should be careful to handle bigon case as in figure 3.3. If we restrict G contains only the faces whose valency(or degree) is strictly greater than two. The corner notation $c(e_i,e_j)$, referred by edges, can be well-defined and we have the following formula immediately.

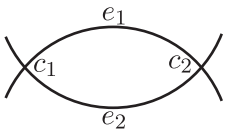

Figure 3.3: $c(e_1,e_2)$ cannot determined the corresponding corner

Proposition 3.11. *If G has no bigon faces, we have*

$$\boldsymbol{ec}\left(\sum_{e\in E(G)}a_e e\right)=\sum_{\substack{e_i,e_j\in E(G)\\ e_j\to e_i}}(a_{e_i}-a_{e_j})c(e_i,e_j)$$

The following figure 3.4 and 3.5 show what are the corresponding images of the generators by the corner homomorphsms pictorially.

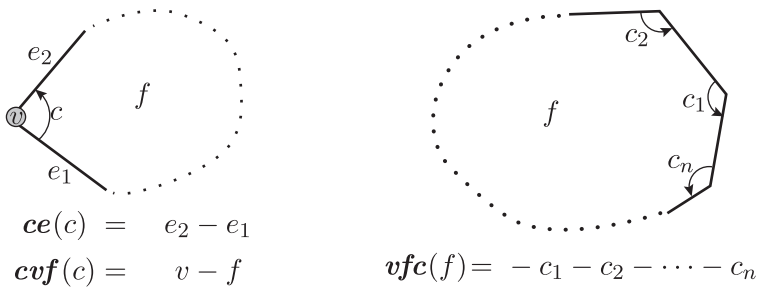

$\boldsymbol{ce}(c) = e_2 - e_1$

$\boldsymbol{cvf}(c) = v - f$

$\boldsymbol{vfc}(f) = -c_1 - c_2 - \cdots - c_n$

Figure 3.4: Corner homomorphisms from corners and faces

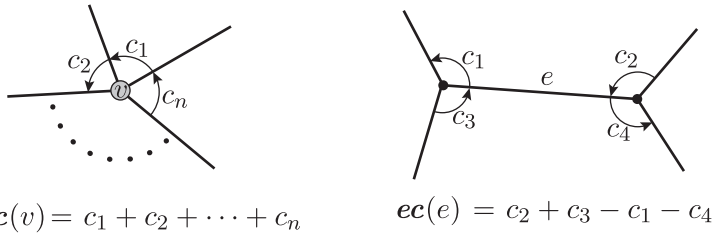

$\boldsymbol{vfc}(v) = c_1 + c_2 + \cdots + c_n$ $\qquad$ $\boldsymbol{ec}(e) = c_2 + c_3 - c_1 - c_4$

Figure 3.5: Corner homomorphisms from vertices and edges

3.3 Corner sequences

The essence of this story is nothing but constructing acyclic chain complexes which is a natural extension of ***cvf*** (or ***ce***) corner homomorphism, called *CVF*-chain complex (or *CE*-chain complex, repectively). Of course, it is possible to prove by direct computation of the corner homomorphisms via analyzing combinatorics of the graph corners. And those things are just fairly routine exercises for homological algebra.

Meanwhile, once we observe that these chain complexes are exactly same with a diagram exact sequences (in section 3.1) on a certain type of induced graphs of G, everything is clear and nothing to compute directly.

3.3.1 *CE*- and *CVF*- chain complex

Definition 3.12. We define the following sequences $CVF(G)$ and $CE(G)$ called *CVF*- or *CE*- chain of G.

$$CVF(G) \quad : \quad 0 \longrightarrow \mathbb{Z} \xhookrightarrow{\iota} \mathscr{E} \xrightarrow{\boldsymbol{ec}} \mathscr{C} \xrightarrow{\boldsymbol{cvf}} \mathscr{VF} \xrightarrow{\epsilon} \mathbb{Z} \longrightarrow 0$$

$$CE(G) \quad : \quad 0 \longrightarrow \mathbb{Z} \xhookrightarrow{\iota} \mathscr{VF} \xrightarrow{\boldsymbol{vfc}} \mathscr{C} \xrightarrow{\boldsymbol{ce}} \mathscr{E} \xrightarrow{\epsilon} \mathbb{Z} \longrightarrow 0$$

where ϵ is the augmentation map

$$\epsilon : \mathscr{E} \longrightarrow \mathbb{Z} \qquad \text{by} \qquad \sum_{e\in E(G)} a_e e \longmapsto \sum_{e\in E(G)} a_e$$

$$\epsilon : \mathscr{VF} \longrightarrow \mathbb{Z} \qquad \text{by} \qquad \sum_{v\in V(G)} a_v v + \sum_{f\in F(G)} a_f f \longmapsto \sum_{v\in V(G)} a_v + \sum_{f\in F(G)} a_f$$

and ι is the dual map of the augmentation ϵ.

$$\iota : \mathbb{Z} \longhookrightarrow \mathscr{E} \qquad \text{by} \qquad 1 \longmapsto \sum_{e\in E(G)} e$$

$$\iota : \mathbb{Z} \longhookrightarrow \mathscr{VF} \qquad \text{by} \qquad 1 \longmapsto \sum_{v\in V(G)} v + \sum_{f\in (G)} f$$

We can easily check that the composition of the homomorphisms at each degree in the above sequence is the zero map and those sequeces are actually chain complexes. But we don't need to prove these arguments because of the relationship with the induced graphs described in the following section. And furthermore we obtain the following main theorem trivially.

Theorem 3.13. *CVF(G) and CE(G) are acyclic chain complexes.*

3.3.2 Medial and cubical graph

Let G be a plane graph and G^* be a dual graph of G. It is convinient to distinguish the vertices of G as black color and the vertices of G^* as white color, like in figure 3.6.

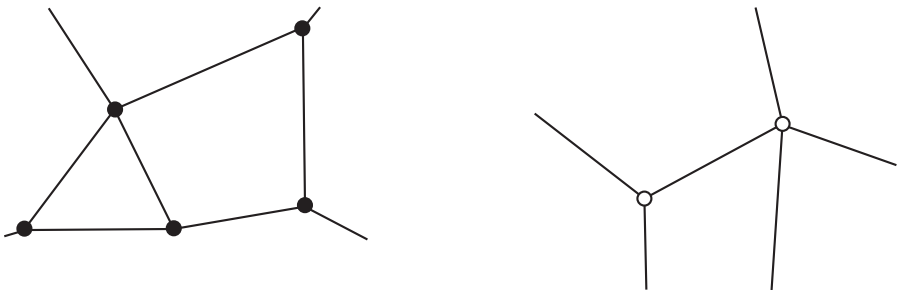

(a) a graph G (b) A dual graph G^*

Figure 3.6: A local picture of G and dual G^*

And consider $G \bigcup G^*$ and define $\mathbf{E}(G) := \left(G \bigcup G^*\right)^c$ as the complement of $G \bigcup G^*$ in the ambient plane in figure 3.7. And then, we construct the following two types of induced graphs.

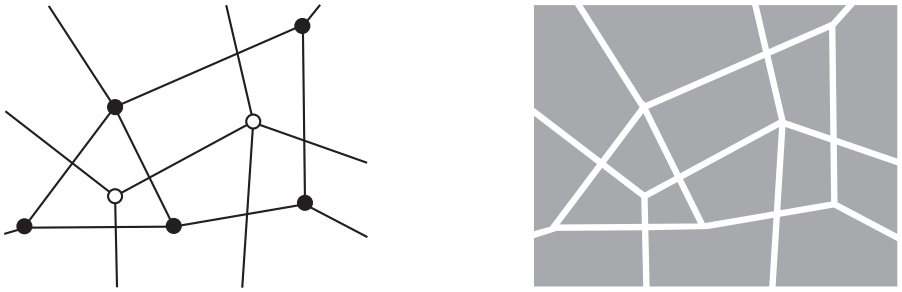

Figure 3.7: $G \bigcup G^*$ and $\mathbf{E}(G)$

Definition 3.14. A *medial graph* G, denoted by G^{med}, is a graph whose vertex set $V(G^{med})$ is given by $E(G) \bigcap E(G^*)$ and which is homotopy equivalent to $V(G^{med}) \bigcup \mathbf{E}(G)$.

By the definition, each edge of G^{med} is given by the deformation retract of the connected component of $\mathbf{E}(G)$ like in figure 3.8a and the obvious propositions follow.

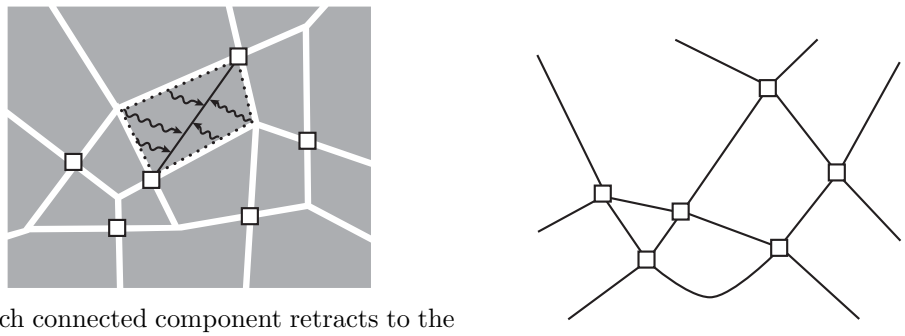

(a) Each connected component retracts to the edge joining vertices in $V(G^{med})$

(b) G^{med}

Figure 3.8: Medial graph of G

Proposition 3.15. *There is 1-1 correspondence between $E(G^{med})$ and the connected components of $\mathbf{E}(G)$.*

Proposition 3.16. *G^{med} is a 4-valent graph.*

Proof. Each vertex in $V(G^{med})$ is obtained by the intersection between two edges, so incident to 4 (half) edges and 4 faces. Therefore the point connect with only 4-connected components in $\mathbf{E}(G)$ join with as in figure 3.8. □

In similar way, we also define another induced graph G^{cub}.

Definition 3.17. A *cubical graph* G, denoted by G^{cub}, is a graph whose vertex set $V(G^{cub})$ is given by $V(G) \bigcup F(G)$ and which is homotopy equivalent to $V(G^{cub}) \bigcup \mathbf{E}(G)$, as in figure 3.9

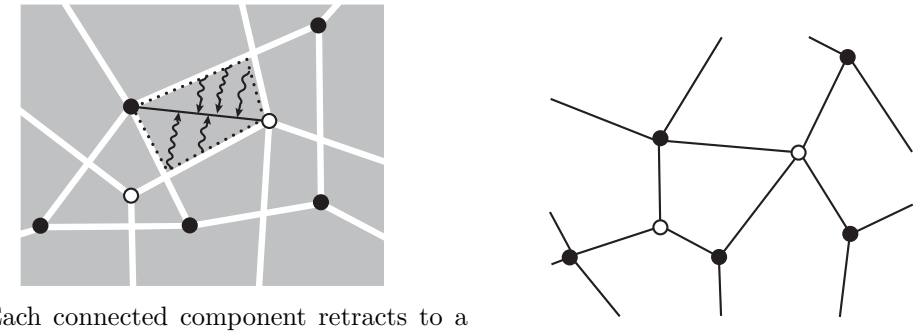

(a) Each connected component retracts to a edge of G^{cub}

(b) G^{cub}

Figure 3.9: Cubical graph of G

Similarily, obvious propositions also follow.

Proposition 3.18. *There is 1-1 correspondence between $E(G^{cub})$ and the connected components of $\mathbf{E}(G)$.*

Proposition 3.19. *G^{cub} and G^{med} are dual graph of each other as in figure 3.10.*

Proposition 3.20. *G^{cub} admits only 4-valent faces, i.e. is 2-dimensional cube complex.*

Proposition 3.21. *G^{cub} is bipartite graph.*

Proof. Since $V(G^{cub}) = V(G) \bigcup F(G)$, There are two color (black and white) of vertices, and $\mathbf{E}(G)$ connects only black vertex and white vertex □

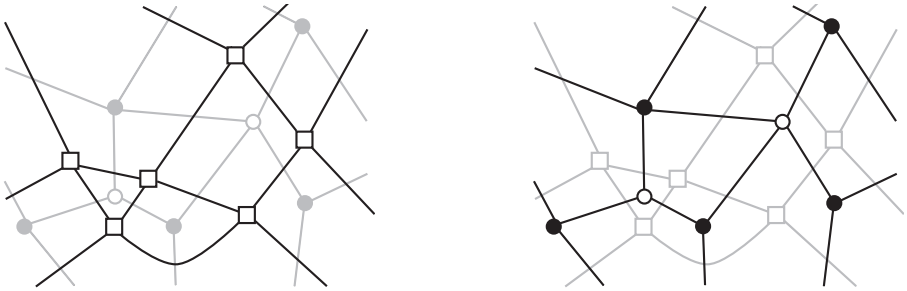

(a) G^{med} and its dual (b) G^{cub} and its dual

Figure 3.10: G^{med} and G^{cub}

3.3.3 Corner sequences and induced graph

Let the set of connected components in $\mathbf{E}(G)$ be denoted by $\widetilde{\mathbf{E}}(G)$.

Proposition 3.22. *We have the following correspondences.*

$$\begin{array}{ccccccc} E(G)\bigcap E(G^*) & \longleftrightarrow & E(G) & \longleftrightarrow & F(G^{cub}) & \longleftrightarrow & V(G^{med}) \\ \widetilde{\mathbf{E}}(G) & \longleftrightarrow & C(G) & \longleftrightarrow & E(G^{cub}) & \longleftrightarrow & E(G^{med}) \\ & & V(G)\bigcup F(G) & \longleftrightarrow & V(G^{cub}) & \longleftrightarrow & F(G^{med}) \end{array}$$

Proof. We can observe the each elements in $\widetilde{\mathbf{E}}(G)$ contains one corner of G as well as exactly one edge of G^{cub} or G^{med}, as in Figure 3.11. With proposition 3.19, figure 3.7 and 3.10 show the above corrrespondence obviously. □

Proof of theorem 3.13. Note that the orientation of the edges in G^{cub} and G^{med} in figure 3.11 agree with corner homomorphsims $\boldsymbol{ce}$ and $\boldsymbol{cvf}$.

$$\begin{array}{lcccccccccccc} \widetilde{\mathcal{C}(G^{cub})} & : & 0 & \longrightarrow & \ker d_2 & \overset{\iota}{\hookrightarrow} & \mathcal{C}_2(G^{cub}) & \overset{d_2}{\longrightarrow} & \mathcal{C}_1(G^{cub}) & \overset{d_1}{\longrightarrow} & \mathcal{C}_0(G^{cub}) & \overset{\epsilon}{\longrightarrow} & \mathbb{Z} \longrightarrow 0 \\ & & & & \| & & \| & & \| & & \| & & \| \\ CVF(G) & : & 0 & \longrightarrow & \mathbb{Z} & \overset{\iota}{\hookrightarrow} & \mathscr{E} & \overset{\boldsymbol{ec}}{\longrightarrow} & \mathscr{C} & \overset{\boldsymbol{cvf}}{\longrightarrow} & \mathscr{VF} & \overset{\epsilon}{\longrightarrow} & \mathbb{Z} \longrightarrow 0 \end{array}$$

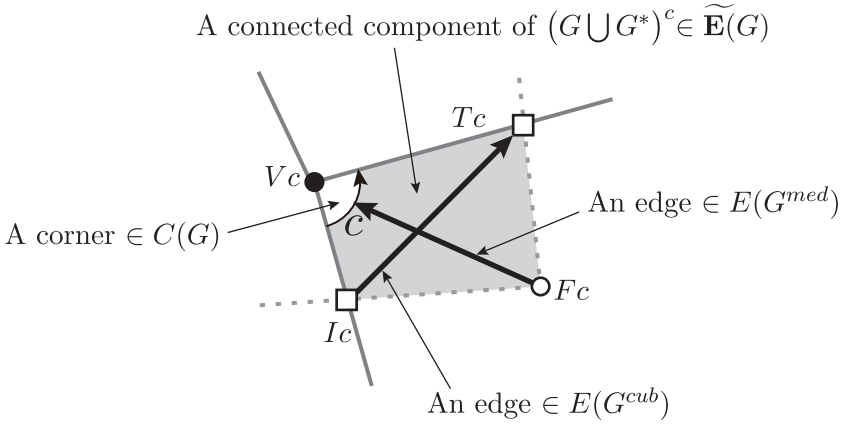

Figure 3.11: $E(G^{med})$, $E(G^{cub})$, $C(G)$ and $\widetilde{\mathbf{E}}(G)$

$$\begin{array}{lcccccccccccc}
\widetilde{\mathcal{C}(G^{med})} & : & 0 & \longrightarrow & \ker d_2 & \xhookrightarrow{\iota} & \mathcal{C}_2(G^{med}) & \xrightarrow{d_2} & \mathcal{C}_1(G^{med}) & \xrightarrow{d_1} & \mathcal{C}_0(G^{med}) & \xrightarrow{\epsilon} & \mathbb{Z} \longrightarrow 0 \\
 & & & & \| & & \| & & \| & & \| & & \| \\
CE(G) & : & 0 & \longrightarrow & \mathbb{Z} & \xhookrightarrow{\iota} & \mathscr{VF} & \xrightarrow{\boldsymbol{vfc}} & \mathscr{C} & \xrightarrow{\boldsymbol{ce}} & \mathscr{E} & \xrightarrow{\epsilon} & \mathbb{Z} \longrightarrow 0
\end{array}$$

$CE(G)$ and $CVF(G)$ is same with $\widetilde{\mathcal{C}(G^{med})}$ and $\widetilde{\mathcal{C}(G^{cub})}$, obviously, acylic. $\square$

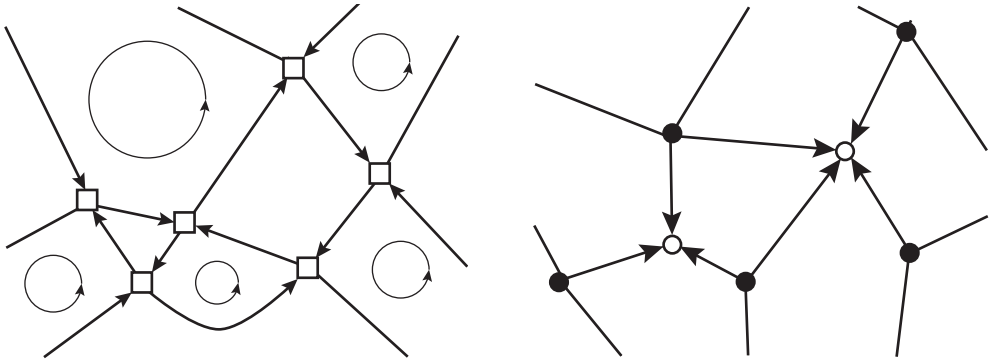

Figure 3.12: Edge orientation of G^{med} and G^{cub}

Medial graph is usually considered by induced graph of knot diagram (vertex-face graph). Cubical graph is a sort of 2-dimensional cube complex, nothing but just dual of medial graph(radial graph).

3.4 $\mathbb{Z}_2$-coefficient and corner parity systems

We can also define *CE*- and *CVF*- cochain complexes as dual.

$$CVF^*(G) \quad : \quad 0 \longrightarrow \mathbb{Z} \xhookrightarrow{\iota} \mathscr{E}^* \xrightarrow{\boldsymbol{ec}^*} \mathscr{C}^* \xrightarrow{\boldsymbol{cvf}^*} \mathscr{VF}^* \xrightarrow{\epsilon} \mathbb{Z} \longrightarrow 0$$

$$CE^*(G) \quad : \quad 0 \longrightarrow \mathbb{Z} \xhookrightarrow{\iota} \mathscr{VF}^* \xrightarrow{\boldsymbol{vfc}^*} \mathscr{C}^* \xrightarrow{\boldsymbol{ce}^*} \mathscr{E}^* \xrightarrow{\epsilon} \mathbb{Z} \longrightarrow 0$$

Cosider *CVF*-cochain complex with $\mathbb{Z}_2$-coefficent.

$$CVF(G)^*_{\mathbb{Z}_2} = CVF(G^*) \otimes \mathbb{Z}_2$$

We note that $\mathscr{C}^* \otimes \mathbb{Z}_2$ in $CVF(G)^*_{\mathbb{Z}_2}$ is free $\mathbb{Z}_2$-module generated by maps $\mathscr{C} \longrightarrow \mathbb{Z}_2$. Moreover, $\boldsymbol{cvf}^*$ is the following property by the definition.

$$\boldsymbol{cvf}^*(\alpha)(x) = \sum_{c \sim x} \alpha(c) \tag{3.2}$$

where x is a face or a vertex in G. Note the fact that the preimage of the following element P in $\mathscr{VF}^*$

$$\begin{aligned} &1)\ P(v) \equiv \deg(v) \pmod 2 && \text{for all } v \in V(G) \\ &2)\ P(v) \equiv 0 \pmod 2 && \text{for all } f \in F(G) \end{aligned}$$

If we consider $\mathbb{Z}_2$ as multiplicative group of $\{+1, -1\}$, $(\boldsymbol{cvf}^*)^{-1}(P)$ is exactly satisfying the condition of corner parity system 2.12. Now we can prove theorem 2.2 and 3.4 in section

proof of theorem 2.13. The existence of preimage $(\boldsymbol{cvf}^*)^{-1}(P)$ depends only on the next coboundary map $\epsilon(P) = 0$ because of chain complex. The number of odd degree vertices is always 0 in $\mathbb{Z}_2$ for all graphs since the following handshaking lemma.

$$\sum_{v \in V(G)} \deg(v) = 2|E(G)|$$

□

proof of theorem 2.15. Let P_1 and P_2 be two different corner parity systems. Both are contained in same coset $(\boldsymbol{cvf}^*)^{-1}(P)$ in $\mathscr{C}^*$. Since $\ker(\boldsymbol{cvf}^*)$ act on each coset transitively, $\mathrm{Im}(\boldsymbol{ec}^*)$ also act there. In other word, we can always find the element in $\mathcal{E}^*$ from P_1 to P_2. Obviously, $\mathcal{E}^*$ action does not change every shape parameter of the octahedral decomposition because shape parameters is the ratio of adjacent edges. □

Chapter 4

Volume potential function for knotted graph

4.1 Volume potential function for knotted graph

By this time, we have investigate hyperbolic structure for knotted graph complements via analyzing a specific triangulation. The main purpose using such generalized octahedral decomposition is to obtain the following theorem.

Theorem 4.1. *Let G be an hyperbolic knotted graph. Define a complex multi-valued function V_G is the summation of* Li_2 *as the substitution rule depicted in figure 4.1. If the solution set $\mathcal{S}$ of their critical equations is not empty, then*

$$\mathrm{Im}\widehat{V}_G(\zeta) = \mathrm{vol}(G),$$

where $\widehat{V}_G(\zeta)$ is the maximal evaluation on $\mathcal{S}$,

Remark 4.2. Considering theorem 1.8, we can say $\widehat{V}_G(\zeta) = \widetilde{V}_G(\widetilde{\zeta})$ as the theorem in introduction of this dissertation.

Remark 4.3. This theorem is a kind of direct generalization for optimistic limit of Kashaev invariant in [2]. As far as I know, it is not clear yet what is the right definition of Kashaev invariant or a quantum invariant for fully general knotted graph case. So volume potential function of knotted graph in theorem 4.1 is not interpreted yet as an optimistic limit of something. Nevertheless, this theorem is an evidence for quantum invariant of knotted graph beyond quantum spin network.

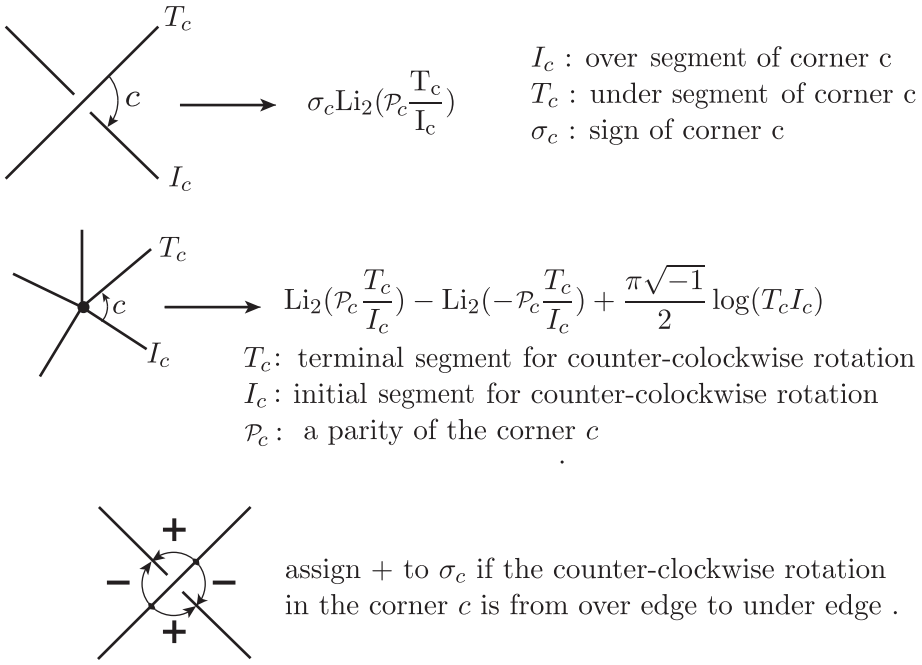

Figure 4.1: Substitution rule for the knotted graph diagram

Proof. Hyperbolicity equations consist of edge-gluing equations and meridian equations. Recall section 2.2.2, there are $\alpha, \beta, \gamma, \delta$ edges. γ and δ edges are satisfied by edge parametrization and critical equations for non-vertex segments gives meridian equations exactly like [2].

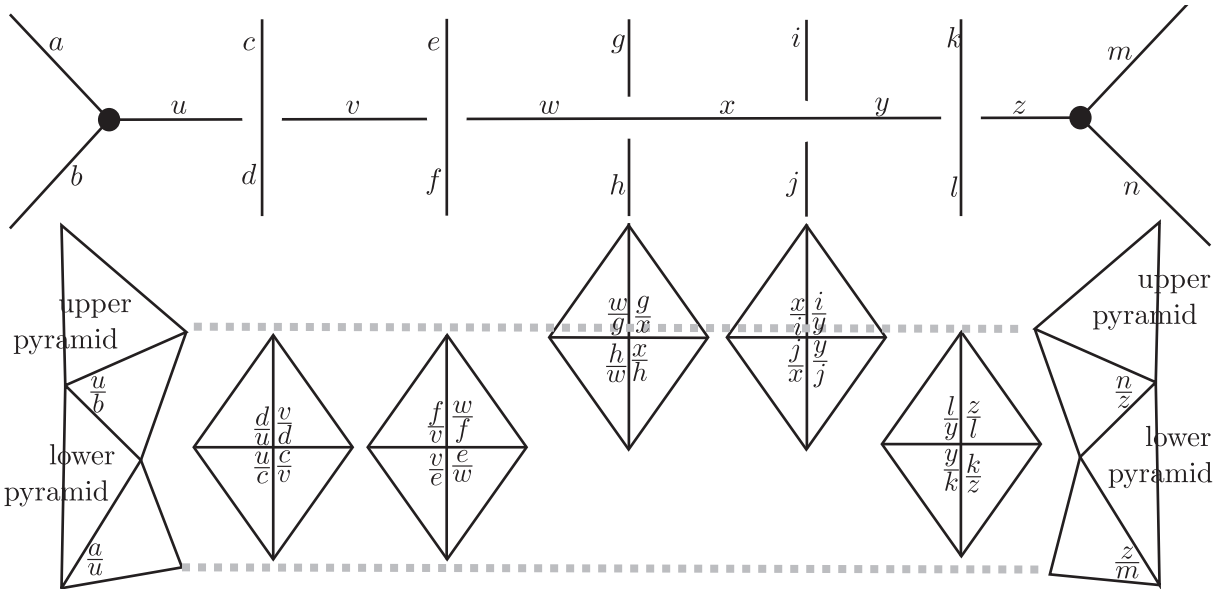

Figure 4.2: Comparing diagram and (annular) cusp shape

Let us see the cusp development for the case in figure 2.8. We should check α edges and β edges but most of them are exactly same formulation with the case of [2]. The only remaining part is only for the case of vertex-segments in figure 4.3.

Potential function for vertex-segments like in above figure is

$$V_x = \mathrm{Li}_2(\frac{d}{x}) - \mathrm{Li}_2(\frac{b}{x}) + \mathrm{Li}_2(\frac{a}{x}) - \mathrm{Li}_2(-\frac{a}{x}) + \mathrm{Li}_2(\frac{x}{c}) - \mathrm{Li}_2(-\frac{x}{c}) + \pi\sqrt{-1}\log x$$

Compute the critical equation for V_x.

$$\exp(x\frac{\partial V_x}{\partial x}) = -\frac{(1-d/x)(1-a/x)(1+x/c)}{(1-b/x)(1+a/x)(1-x/c)}$$

This gives exactly same with edge equation in figure 4.3. And the meridian equation at the segment is

$$\begin{aligned}\frac{x}{c}(\nu)^{-1}\frac{a}{x}(\lambda)^{-1} &= \frac{x}{c}\frac{a}{x}((\frac{x}{c})'(\frac{x}{c})'')^{-1}((\frac{a}{x})'(\frac{a}{x})'')^{-1} \\ &= \frac{x}{c}\frac{a}{x}(-\frac{x}{c})^{-1}(-\frac{a}{x})^{-1} = 1\end{aligned}$$

Summarizing all of these thing, edge parametrization and critical equation of our potential function of figure 4.1 solve the hyperbolicity equation of the given knotted graph complements.

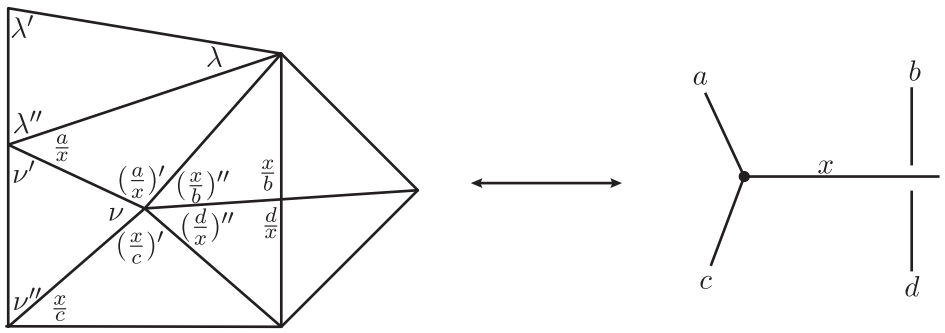

Figure 4.3: Cusp shape of a vertex-segment

By corollary 1.6, It is suffice to show critical equation is equivalent to Hyperbolicity equations. We can conclude that the potential function defined by the rule 4.1 have hyperbolic volume as maximal evaluation on $\mathcal{S}$. □

4.2 Example for tetrahedron graph

At first, we need a corner parity system. Let us consider a graph diagram with a corner parity system and make potential function V.

then we have critical equations. and

$$\begin{aligned} V(z) = \quad & +\mathrm{Li}_2(\tfrac{z_5}{z_4}) - \mathrm{Li}_2(-\tfrac{z_5}{z_4}) + \mathrm{Li}_2(\tfrac{z_4}{z_6}) - \mathrm{Li}_2(-\tfrac{z_4}{z_6}) + \mathrm{Li}_2(\tfrac{z_6}{z_5}) - \mathrm{Li}_2(-\tfrac{z_6}{z_5}) \\ & -\mathrm{Li}_2(\tfrac{z_2}{z_1}) + \mathrm{Li}_2(-\tfrac{z_2}{z_1}) + \mathrm{Li}_2(\tfrac{z_1}{z_3}) - \mathrm{Li}_2(-\tfrac{z_1}{z_3}) + \mathrm{Li}_2(\tfrac{z_5}{z_1}) - \mathrm{Li}_2(-\tfrac{z_5}{z_1}) \\ & -\mathrm{Li}_2(\tfrac{z_1}{z_6}) + \mathrm{Li}_2(-\tfrac{z_1}{z_6}) + \mathrm{Li}_2(\tfrac{z_3}{z_2}) - \mathrm{Li}_2(-\tfrac{z_3}{z_2}) - \mathrm{Li}_2(\tfrac{z_2}{z_4}) + \mathrm{Li}_2(-\tfrac{z_2}{z_4}) \\ & +\mathrm{Li}_2(\tfrac{z_6}{z_2}) - \mathrm{Li}_2(-\tfrac{z_6}{z_2}) - \mathrm{Li}_2(\tfrac{z_4}{z_3}) + \mathrm{Li}_2(-\tfrac{z_4}{z_3}) + \mathrm{Li}_2(\tfrac{z_3}{z_5}) - \mathrm{Li}_2(-\tfrac{z_3}{z_5}) \end{aligned}$$

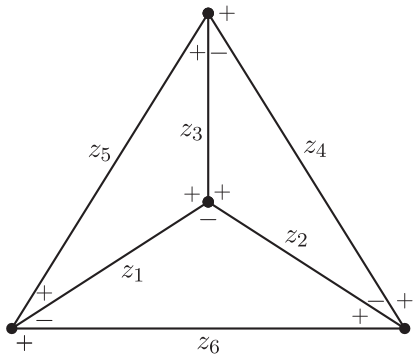

Figure 4.4: Tetrahedron graph diagram with corner parity system

$$\mathcal{H} = \left\{ \begin{array}{l} \exp(z_1\frac{\partial V}{z_1}) = \frac{(z_1-z_5)(z_1+z_2)(z_1+z_3)(z_1-z_6)}{(z_1+z_5)(z_1-z_2)(z_1-z_3)(z_1+z_6)} = 1, \\ \exp(z_1\frac{\partial V}{z_2}) = \frac{(z_2-z_3)(z_2-z_6)(z_2-z_1)(z_2-z_4)}{(z_2+z_3)(z_2+z_6)(z_2+z_1)(z_2+z_4)} = 1, \\ \exp(z_1\frac{\partial V}{z_3}) = \frac{(z_3-z_5)(z_3-z_2)(z_3+z_1)(z_3-z_4)}{(z_3+z_5)(z_3+z_2)(z_3-z_1)(z_3+z_4)} = 1, \\ \exp(z_1\frac{\partial V}{z_4}) = \frac{(z_4+z_3)(z_4-z_6)(z_4+z_5)(z_4-z_2)}{(z_4-z_3)(z_4+z_6)(z_4-z_5)(z_4+z_2)} = 1, \\ \exp(z_1\frac{\partial V}{z_5}) = \frac{(z_5-z_4)(z_5-z_1)(z_5+z_3)(z_5+z_6)}{(z_5+z_4)(z_5+z_1)(z_5-z_3)(z_5-z_6)} = 1, \\ \exp(z_1\frac{\partial V}{z_6}) = \frac{(z_6+z_1)(z_6-z_4)(z_6+z_2)(z_6+z_5)}{(z_6-z_1)(z_6+z_4)(z_6-z_2)(z_6-z_5)} = 1 \end{array} \right\} \tag{4.1}$$

Solving the equations , we can get the solutions for $\mathcal{H}$ as the following.

$$\boldsymbol{\zeta} = (\zeta_1, \zeta_2, \zeta_3, \zeta_4, \zeta_5, \zeta_6) \in \mathcal{S},$$

where

$$\begin{aligned} \zeta_4 = & -\frac{\zeta_1\zeta_2+(1-\sqrt{-1})\zeta_2\zeta_3+\sqrt{-1}\zeta_1\zeta_3}{(1+\sqrt{-1})\zeta_1-\sqrt{-1}\zeta_2+\zeta_3}, \\ \zeta_5 = & -\frac{\sqrt{-1}\zeta_1\zeta_2+\zeta_2\zeta_3+(-1+\sqrt{-1})\zeta_1\zeta_3}{\zeta_1-(1+\sqrt{-1})\zeta_2-\sqrt{-1}\zeta_3}, \\ \zeta_6 = & \frac{(1+\sqrt{-1})\zeta_1\zeta_2+\zeta_2\zeta_3+\sqrt{-1}\zeta_1\zeta_3}{\zeta_1-\sqrt{-1}\zeta_2+(1-\sqrt{-1})z_3} \end{aligned}$$

We can check that compendsated evaulation $\widehat{V}_D(\boldsymbol{\zeta})$ is constant for $\forall\zeta_1, \zeta_2, \zeta_3 \in \mathbb{C}^*$ by numerical test,

$$\widehat{V}_D(\boldsymbol{\zeta}) = \pm 7.327724.. = \mathrm{vol}(S^3 - \text{☮})$$

Bibliography

[1] Dan Archdeacon. Topological graph theory: a survey. *Congressus Numerantium. A Conference Journal on Numerical Themes*, 115:5–54, 1996. Surveys in graph theory (San Francisco, CA, 1995).

[2] Jinseok Cho, Hyuk Kim, and Seonhwa Kim. Optimistic limits of kashaev invariants and complex volumes of hyperbolic links. January 2013.

[3] Jinseok Cho and Jun Murakami. The complex volumes of twist knots via colored jones polynomials. *Journal of Knot Theory and its Ramifications*, 19(11):1401–1421, 2010.

[4] Jinseok Cho and Jun Murakami. Optimistic limits of the colored jones polynomials. arXiv e-print 1009.3137, September 2010.

[5] Jinseok Cho, Jun Murakami, and Yoshiyuki Yokota. The complex volumes of twist knots. *Proceedings of the American Mathematical Society*, 137(10):3533–3541, 2009.

[6] Tudor Dimofte and Sergei Gukov. Quantum field theory and the volume conjecture. In *Chern-Simons gauge theory: 20 years after*, volume 50 of *AMS/IP Stud. Adv. Math.*, page 19–42. Amer. Math. Soc., Providence, RI, 2011.

[7] Tudor Dimofte, Sergei Gukov, Jonatan Lenells, and Don Zagier. Exact results for perturbative chern-simons theory with complex gauge group. *Communications in Number Theory and Physics*, 3(2):363–443, 2009.

[8] Tudor D. Dimofte and Stavros Garoufalidis. The quantum content of the gluing equations. February 2012.

[9] Stefano Francaviglia. Algebraic and geometric solutions of hyperbolicity equations. *Topology and its Applications*, 145(1-3):91–118, 2004.

[10] Sergei Gukov. Three-dimensional quantum gravity, chern-simons theory, and the a-polynomial. arXiv e-print hep-th/0306165, June 2003. Commun.Math.Phys. 255 (2005) 577-627.

[11] Allen Hatcher. *Algebraic topology*. Cambridge University Press, Cambridge, 2002.

[12] Damian Heard, Craig Hodgson, Bruno Martelli, and Carlo Petronio. Hyperbolic graphs of small complexity. *Experimental Mathematics*, 19(2):211–236, 2010.

[13] Michael Kapovich. *Hyperbolic manifolds and discrete groups*, volume 183 of *Progress in Mathematics*. Birkhäuser Boston Inc., Boston, MA, 2001.

[14] R. M. Kashaev. The hyperbolic volume of knots from the quantum dilogarithm. *Letters in Mathematical Physics. A Journal for the Rapid Dissemination of Short Contributions in the Field of Mathematical Physics*, 39(3):269–275, 1997.

[15] Leonard Lewin, editor. *Structural properties of polylogarithms*, volume 37 of *Mathematical Surveys and Monographs*. American Mathematical Society, Providence, RI, 1991.

[16] Feng Luo, Stephan Tillmann, and Tian Yang. Thurston's spinning construction and solutions to the hyperbolic gluing equations for closed hyperbolic 3-manifolds. *Proceedings of the American Mathematical Society*, 141(1):335–350, 2013.

[17] Leonard C. Maximon. The dilogarithm function for complex argument. 459(2039):2807–2819, 2003.

[18] Hitoshi Murakami. An introduction to the volume conjecture. In *Interactions between hyperbolic geometry, quantum topology and number theory*, volume 541 of *Contemp. Math.*, page 1–40. Amer. Math. Soc., Providence, RI, 2011.

[19] Hitoshi Murakami and Jun Murakami. The colored jones polynomials and the simplicial volume of a knot. *Acta Mathematica*, 186(1):85–104, 2001.

[20] Jun Murakami. Volume formulas for a spherical tetrahedron. *Proceedings of the American Mathematical Society*, 140(9):3289–3295, 2012.

[21] Jun Murakami and Akira Ushijima. A volume formula for hyperbolic tetrahedra in terms of edge lengths. *Journal of Geometry*, 83(1-2):153–163, 2005.

[22] Jun Murakami and Masakazu Yano. On the volume of a hyperbolic and spherical tetrahedron. *Comm. Anal. Geom.*, 13(2):379–400, 2005.

[23] Walter D. Neumann. Extended bloch group and the cheeger-chern-simons class. July 2003. Geom. Topol. 8(2004) 413-474.

[24] Walter D. Neumann and Don Zagier. Volumes of hyperbolic three-manifolds. *Topology. An International Journal of Mathematics*, 24(3):307–332, 1985.

[25] Moto-o Takahashi. On the concrete construction of hyperbolic structures of 3-manifolds. *Tsukuba Journal of Mathematics*, 9(1):41–83, 1985.

[26] William Thurston. *The geometry and topology of 3-manifolds.* Lecture notes, Princeton, 1977.

[27] Roland van der Veen. The volume conjecture for augmented knotted trivalent graphs. *Algebraic & Geometric Topology*, 9(2):691–722, 2009.

[28] Jeff Weeks. Computation of hyperbolic structures in knot theory. In *Handbook of knot theory*, page 461–480. Elsevier B. V., Amsterdam, 2005.

[29] Yoshiyuki Yokota. On the volume conjecture for hyperbolic knots. September 2000.

[30] Yoshiyuki Yokota. On the complex volume of hyperbolic knots. *Journal of Knot Theory and its Ramifications*, 20(7):955–976, 2011.

[31] Christian K. Zickert. The volume and chern-simons invariant of a representation. *Duke Mathematical Journal*, 150(3):489–532, 2009.

국문초록

양자불변량의 낙관적 극한법은 카샤에브 부피가설을 풀려는 시도로 개발되었다. 비록 수학적으로 엄밀하게 정식화 하긴 매우 힘들어 보이지만, 이 방법을 통해 쌍곡 매듭의 부피공식을 명시적으로 쓸 수 있으며 쌍곡부피는 매듭다이어그램으로 부터 직접적으로 쓸수있는 잠재함수의 임계값으로 주어지게 된다. 저자는 어떤 특정한 형태의 함수의 임계값이 $PSL(2,\mathbb{C})$-표현의 쌍곡부피가 될 충분조건을 연구하고, 매듭진 그래프의 확장된 팔면체 분할을 통해 매듭진 그래프 여공간의 쌍곡 부피를 구하는 잠재함수를 정의한다.

주요어휘: 부피가설, 양자위상, 쌍곡기하학, 저차원위상, 그래프, 매듭이론
학번: 2004-23257

감사의 글

많은 분들의 지원과 도움 덕분에 여러가지 모자란 점이 많았던 제가 대학원 과정을 무사히 마무리 하고 졸업을 하게 되었습니다. 2004년 가을에 대학원에 입학하여 2013년 가을에 졸업하니 만으로 딱 9 년입니다. 그간 조금이나마 이룬 것이 있다면 그것은 나 자신의 성과라기보다는 저를 믿어주고 도와주신 모든 분들의 것입니다.

가장 먼저 지도교수님인 김혁 교수님의 헌신적인 가르침이 생각납니다. 참다운 수학자의 모습, 학문을 대하는 올바른 태도에 대하여 항상 몸소 모범을 보이셨으며, 제자의 부족한 점을 늘 사랑으로 감싸주셨습니다. 단지 수학뿐만 아니라 삶의 곳곳에 배어 있는 작은 모습과 태도 하나하나로부터 참으로 많은 배움을 얻었으며 일일이 다 열거할 수 없을 만큼 많은 보살핌을 받았습니다. 제가 받은 큰 은혜는 감히 필설로 표현할 수 없으며 앞으로 평생을 갚아도 부족할 것입니다.

부피 가설을 연구하게 되는 데 있어 가장 많은 영향을 준 조진석 씨에게도 감사의 마음을 전합니다. 조진석 씨가 아니었다면, 저의 성격상 제대로 연구 주제를 결정하지 못하고 이리저리 방황하게 되었을 위험이 컸다고 생각합니다. 또한, 언제나 미리 계획된 일을 어기지 않고 잘 지키며 절제된 생활을 하는 모습은 늘 본받고 싶은 점입니다.

항상 아낌없는 조언을 해주시는 조윤희 교수님께도 깊은 감사의 뜻을 전합니다. 아마도 조윤희 교수님이 창안하신 확장 쌍곡 공간에 대한 앞선 연구 결과들이 없었다면 그리고 배우면서 모르는 부분이 있을 때마다 즉시 답을 해주실 수 있는 분이 없었다면 그 개념을 깊이 이해하지 못했을 것이고 제 이론의 바탕이 되는 아이디어를 상상하지 못했을 가능성이 크다고 생각합니다.

전공이 아니어서 어려움이 많았던 이론 물리의 기초에 대해 여러 번에 걸쳐 좋은 강의를 해 주신 이상민 교수님께도 감사의 말씀을 전합니다. 더불어 항상 세미나 시간에 저의 부족한 발표를 경청하고 또 지적해주셨던 정경훈 박사님, 김대용 박사님에게 감사의 마음을 드리고 싶으며, 특히 정경훈 박사님의 양자군에 관련된 표현론 강의는 제게 아주 귀중한 재산이 되었습니다.

논문심사를 해주신 박종일 선생님, 김인강 선생님, 조철현 선생님, Jun Murakami 선생님께도 감사드립니다. 특히 박종일 교수님의 지적과 채찍질은 앞으로 수학자로 살아가는데 있어 큰 지침이 될 것이기에 특별히 더욱 감사드립니다. 아직은 정말 부족한 점이 많지만, 앞으로 부끄럽지 않은 수학자로 바로 설 수 있도록 노력하겠습니다.

어린 시절 친구들이었던 박석원, 이병익, 이정환, 허동필군에게도 특별한 감사의 말을 전하고 싶습니다. 비록 각자 결혼 후에는 자주 만나기는 힘들었지만 믿을 수 있는 친구가 있다는 사실만으로도 흔들리지 않는 큰 힘이 되었습니다. 수학에 관한 이야기를 하는 것이 가장 즐거웠던 친구와 후배들인 윤영호, 김동희, 박주빈, 윤석배, 배영진, 이주현 등에게도 감사하는 마음입니다. 특히 대학원 와서야 만났지만 마치 오랜 시간 이미 만나왔던 것처럼 편안하게 대화를 나누며 많은 걸 교류할수 있었던 윤영호를 만난건 다시 보기 힘든 큰 행운이었다고 생각합니다.

공부하는 와중에 결혼하게 되고 두 아이의 아빠가 되었어도 무사히 학업을 마치게 된 것은 부모님의 도움이 결정적이었습니다. 아들의 눈에 비친 수십 년을 하루같이 근면하고 성실하게 살아가는 아버지의 모습은 그 어떤 금은보화와도 비교할 수 없는 큰 유산이요 축복이라 믿습니다. 거기에 더하여 고단한 몸을 기꺼이 감수하고 아기들을 돌보아주신 어머니의 헌신이 없었다면 학업을 지속하기 정말 어려웠을 것입니다. 항상 자식들이 잘되기만을 바라시는 그 마음, 늘 잊지 않고 큰 은혜에 보답하도록 힘쓸 것입니다.

마지막으로 수많은 어려움을 이겨내는데 가장 큰 버팀목이 되었던 사랑하는 아내 김유리와 건강하게 커가고 있는 우리 딸들 김규린, 김태린에게도 감사를 드립니다. 아내가 없었다면 과연 지금의 내가 있었을까 하는 생각이 듭니다. 철없는 남편 때문에 늘 고생하는 아내에게 다시 한 번 감사하고 또 사랑한다는 말을 꼭 하고 싶습니다.

이제 길었던 학생 시절을 정말로 끝내고, 온실에서 벗어나 진짜 바다로 항해를 떠나야 할 순간이 온 것 같습니다. 그동안 참으로 많은 분들의 보살핌과 지원으로 빚어낸 결과이지만 부족한 능력으로 말미암아 아직은 작디 작은 조각배입니다. 하지만 이를 바탕으로 늘 새로운 것을 배우고 또 다지며 부족한 점을 메꾸어 장차 먼 대양까지 무사히 나아갈 수 있는 튼튼한 배로 바뀔 수 있도록 애쓸것입니다. 그리고 지금껏 받았던 과분한 사랑을 제가 받은 그 이상으로 남들에게 베풀 수 있도록 노력하는 삶이 되기를 마음 깊이 소망합니다.